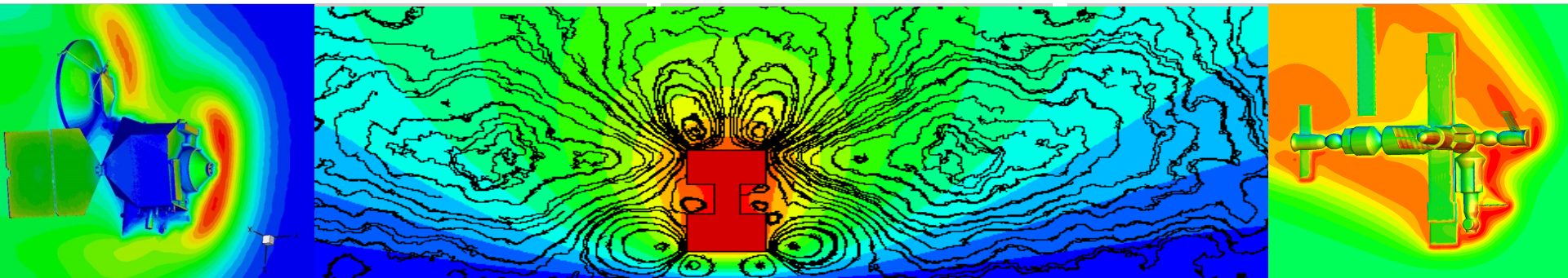


*Exceptional service in the national interest*



## Molecular-Level Simulations of Gas Dynamic Flows

*Michael A. Gallis*

Engineering Sciences Center  
Sandia National Laboratories  
Albuquerque, New Mexico, USA



Sandia National Laboratories is a multi-program laboratory managed and operated by Sandia Corporation, a wholly owned subsidiary of Lockheed Martin Corporation, for the U.S. Department of Energy's National Nuclear Security Administration under contract DE-AC04-94AL85000.

# Collaborators



John Torczynski



Dan Rader



Tim Koehler

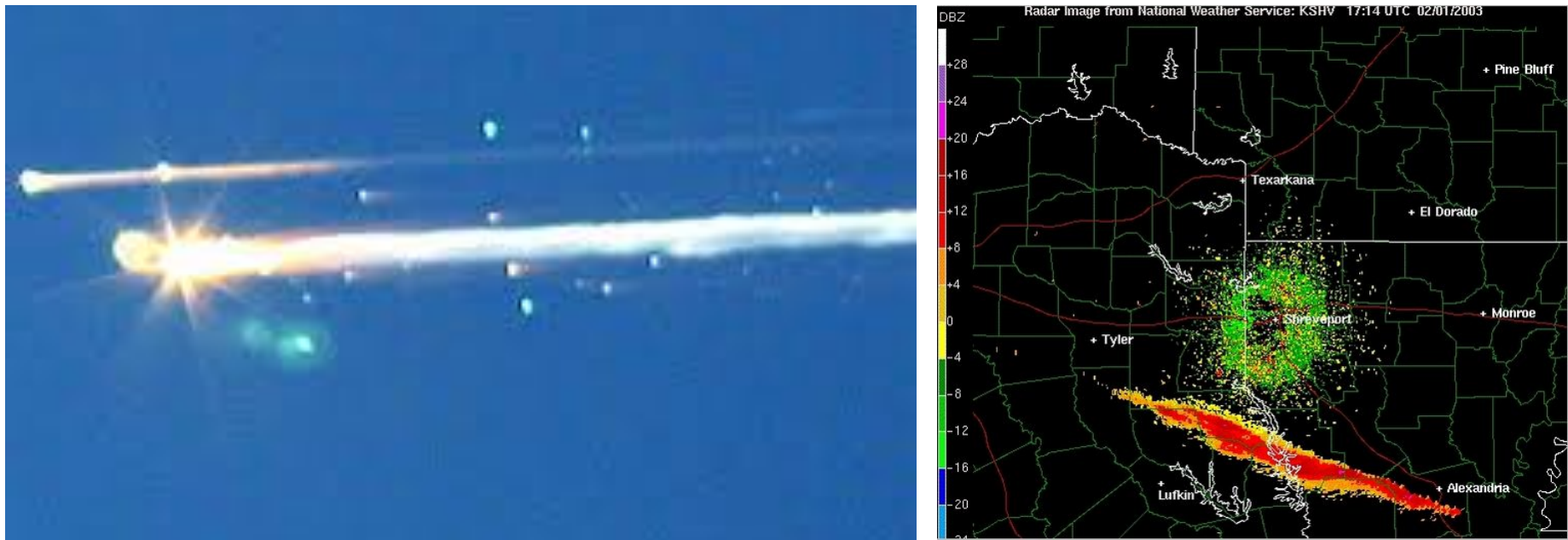


Steve Plimpton

# The Columbia Accident



On February 1<sup>st</sup> 2003 STS-107 with Shuttle orbiter Columbia disintegrated over western Texas, minutes before it was scheduled to land.

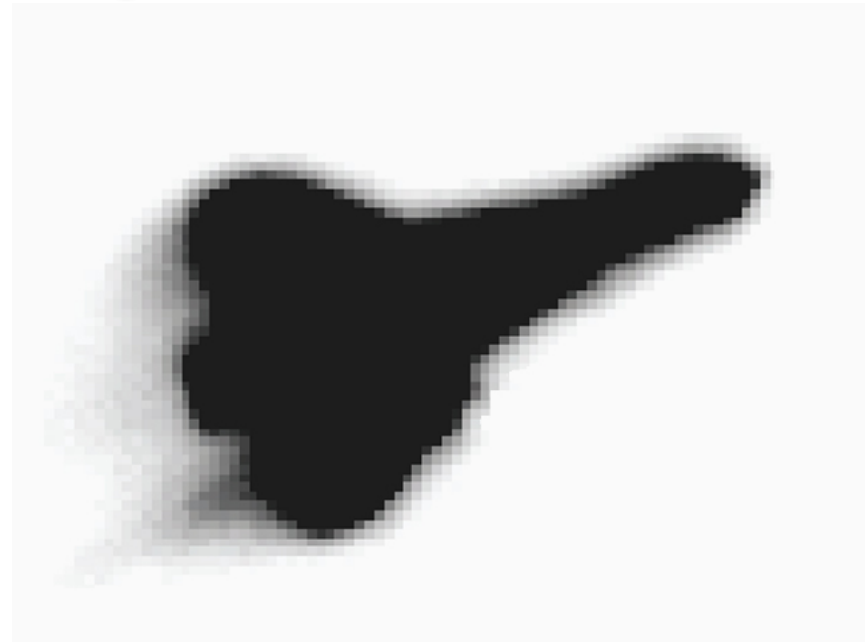


# Foam impact during launch



During the ascent phase a piece of foam insulation broke off from the shuttle's propellant tank and damaged the edge of the shuttle's left wing causing an approximately 10" hole.

# Damage Scenario Investigated



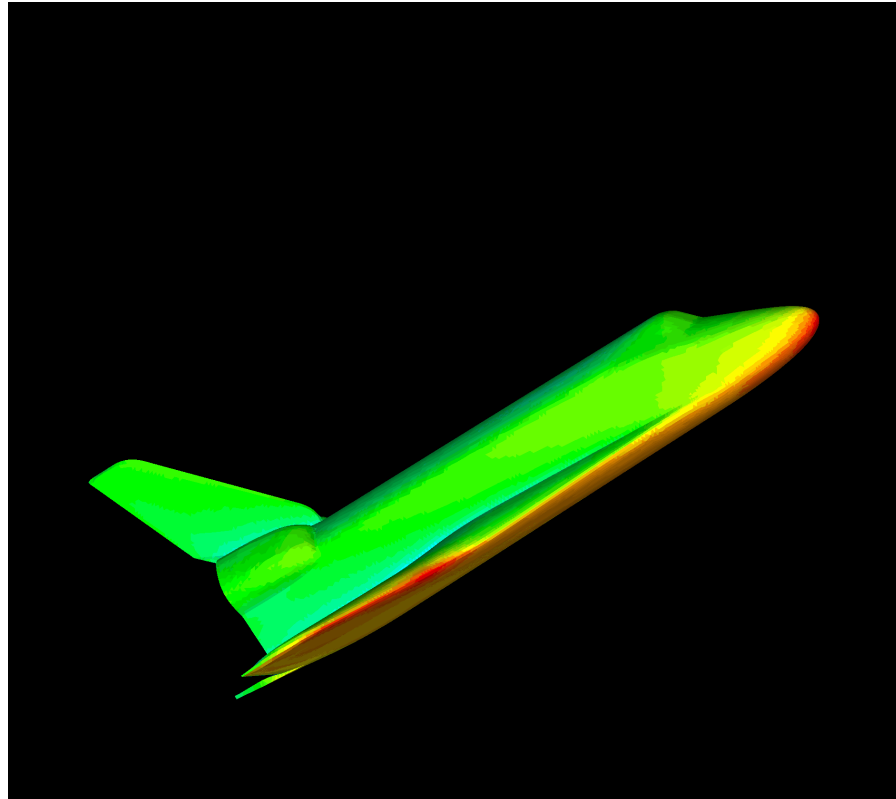
The resulting hole allowed overheated gases to penetrate the wing cavity, compromise its structural integrity, leading to a loss of the vehicle during descent

# Numerical Simulations Supporting the Investigation

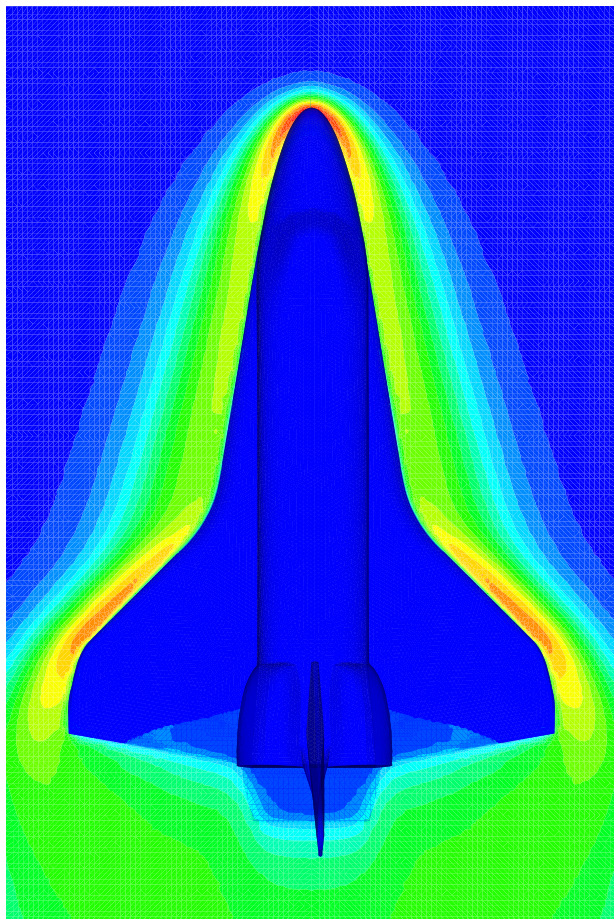
## Simulation conditions

Altitude = 350,000-300,000 ft

Mach Number = 27

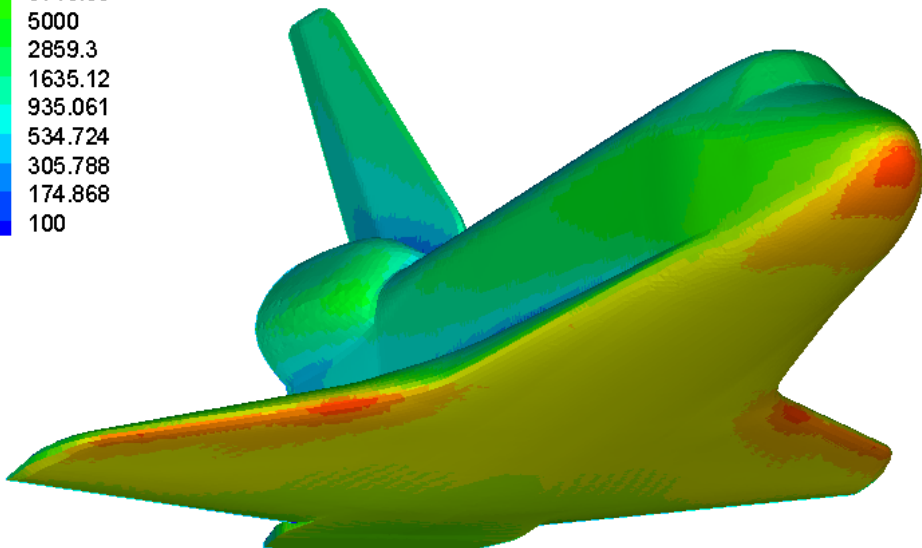


# Temperature and Heating Profile

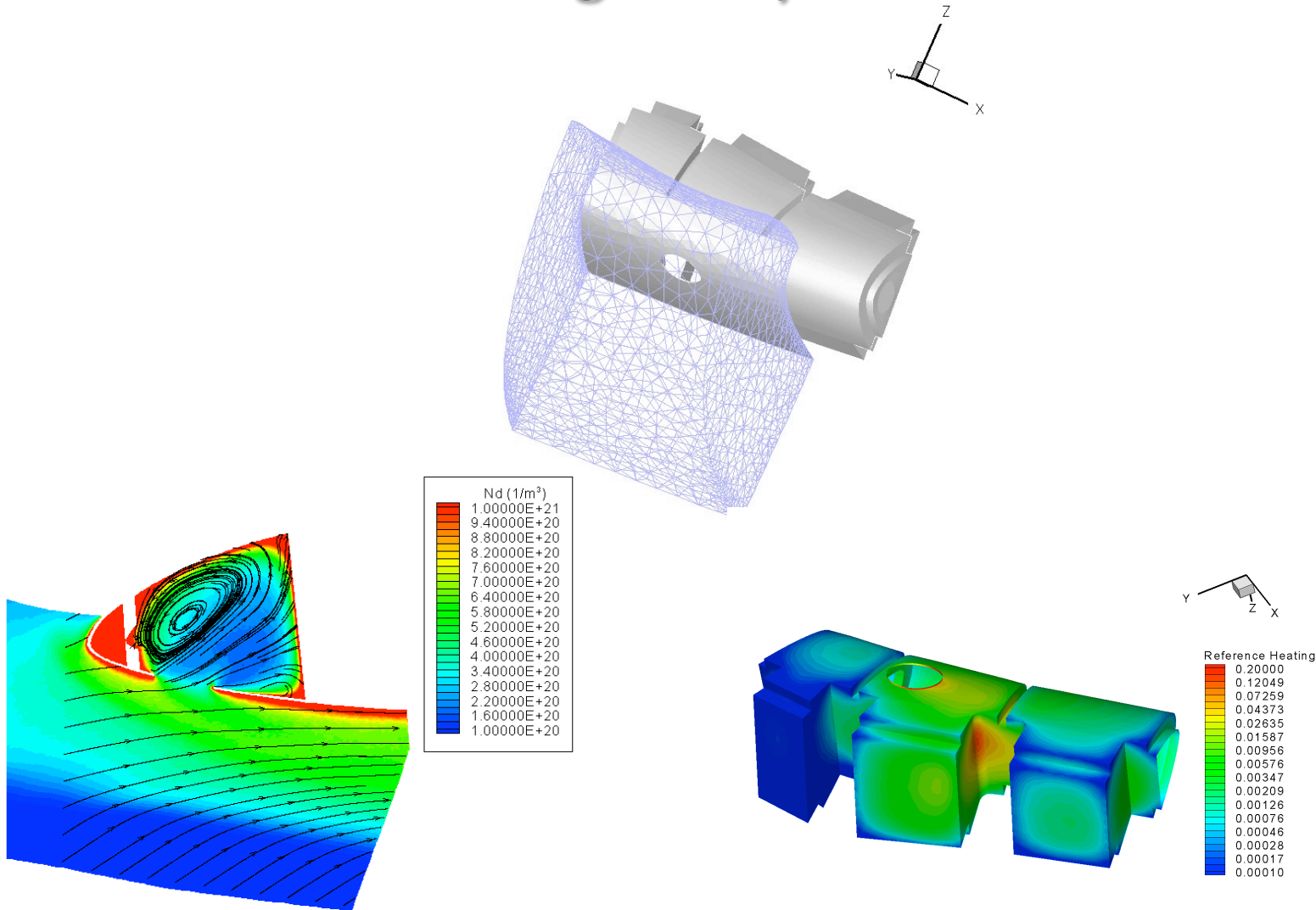


$Q_{Total} (\text{W/m}^2)$

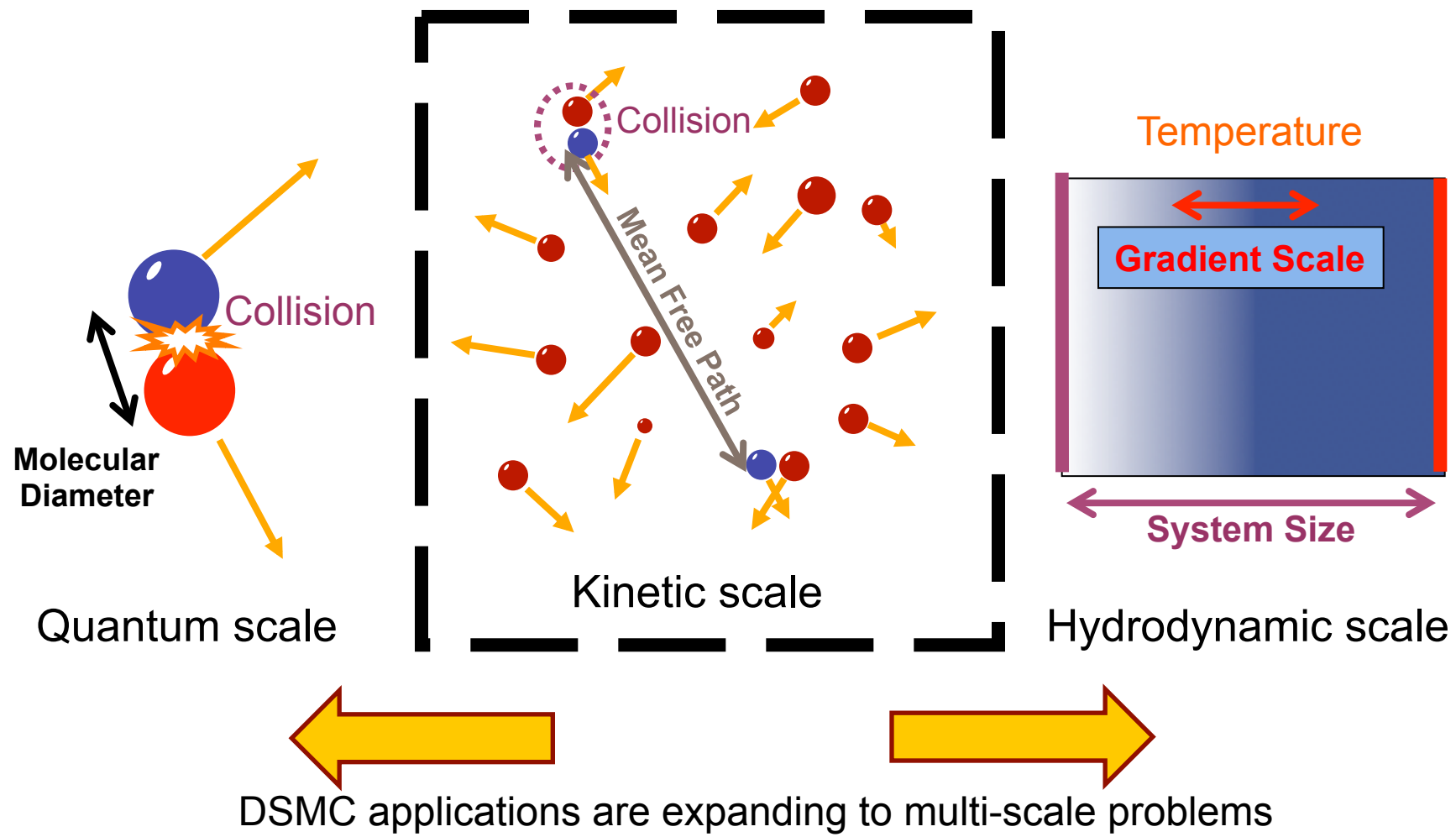
250000
142965
81756.1
46753.1
26736.2
15289.4
8743.39
5000
2859.3
1635.12
935.061
534.724
305.788
174.868
100



# Flow Inside the Wing Cavity



# Length Scales for Dilute Gases



# Boltzmann Equation and the Direct Simulation Monte Carlo Method



Ludwig  
Boltzmann

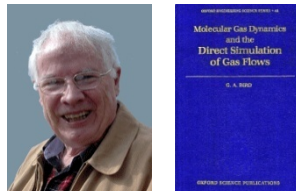
$$\frac{\partial f}{\partial t} + \mathbf{v} \cdot \frac{\partial f}{\partial \mathbf{x}} + \frac{\mathbf{F}}{m} \cdot \frac{\partial f}{\partial \mathbf{v}} = \int_{-\infty}^{\infty} \int_0^{4\pi} (f^* f_1^* - f f_1) |\mathbf{v} - \mathbf{v}_1| \sigma d\Omega d\mathbf{v}_1$$

molecular motion and  
force-induced acceleration

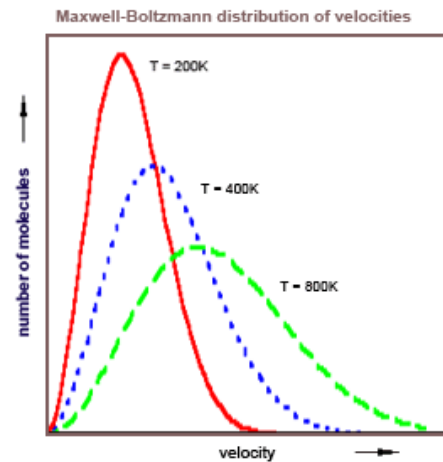
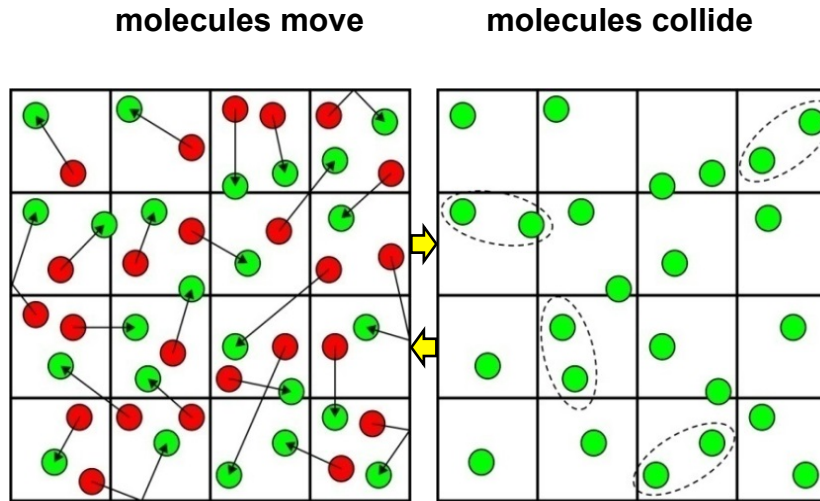
pairwise molecular collisions  
(molecular chaos)



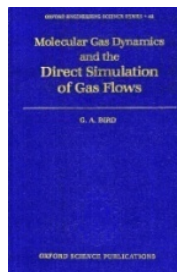
James Clerk  
Maxwell



Graeme Bird  
(1963, 1994)



# Simulating the Kinetic Regime



- “In general, the field of rarefied gas flow problems is still largely unclarified” last sentence from *Elements of Gasdynamics* (1956) by H. W. Liepmann and A. Roshko.
- The Direct Simulation Monte Carlo (**DSMC**) originated in 1963\* by Graeme A. Bird, encouraged by H. Liepmann.
  - \* “G. A. Bird, 'Approach to translational equilibrium in a rigid sphere gas', *Phys. Fluids*, 6, p1518 (1963)”.
- The objective of DSMC is to simulate complicated gas flows using **only collision mechanics of simulated molecules**
- Today, DSMC is the **dominant** numerical algorithm at the kinetic scale
- DSMC applications are expanding to **multi-scale problems** creating new challenges and opportunities.

# Direct Simulation Monte Carlo

## How DSMC works

Computational molecules move ballistically, collide statistically, and interact statistically with surfaces like real molecules

Molecular movement, surface-interaction, and collision are implemented sequentially in the algorithm

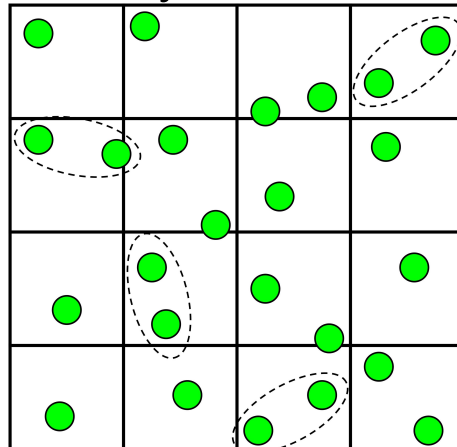
Cell-based molecular statistics (“moments”) are sampled and averaged over many time steps for steady flow

## DSMC issues

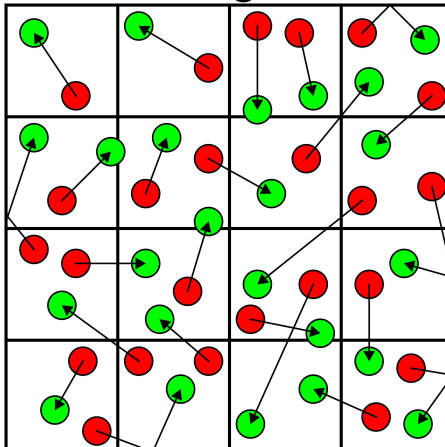
Statistical aspect requires  $O(10^9)$  samples for flows ( $\sim 1$  m/s)

## DSMC is inherently a transient method

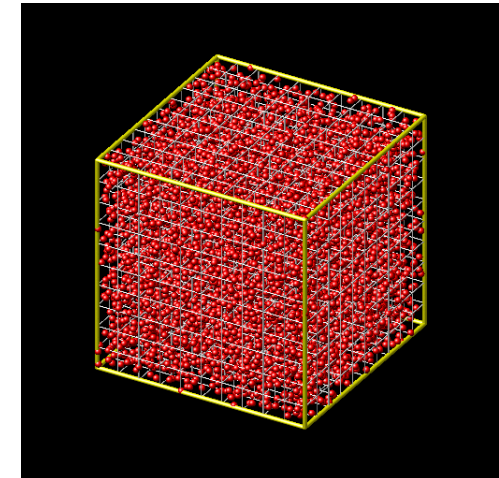
Steady state is the ensemble average of unsteady state moves



+



=



Stochastic binary collisions

Deterministic ballistic move

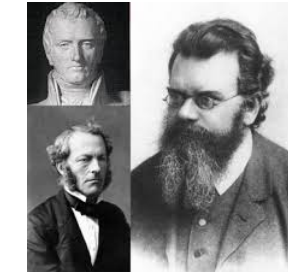
# DSMC vs. Boltzmann Equation

- Instead of solving Newton's laws of motion (Molecular Dynamics), DSMC replaces explicit intermolecular forces with stochastic collisions
- It has been shown that DSMC is **equivalent** to solving the Boltzmann equation (Nambu 1980, Babovsky 1989, Wagner 1992)
- DSMC has been shown to reproduce **exact** known solutions (Chapman-Enskog, Moment Hierarchy) of the Boltzmann equation (Gallis et al. 2004, 2006) for **non-equilibrium** flows
- In fact, DSMC is **superior** to solving the Boltzmann equation
  - DSMC can **model complicated processes** (e.g., polyatomic molecules, chemically reacting flows, ionized flows) for which **Boltzmann-type transport equations are not even known** (Struchtrup 2005)
  - DSMC **includes fluctuations**, which have been shown to be physically realistic (Garcia 1990) but which are **absent from the Boltzmann equation**

**The objective of DSMC is to simulate complicated gas flows using only collision mechanics of simulated molecules in the regime described by the Boltzmann equation**

# Navier-Stokes vs. Boltzmann Equation

- The Navier-Stokes equations for gases can be derived from the Boltzmann equation assuming:
  - Near-equilibrium conditions
  - Local Thermodynamic Equilibrium (LTE)
  - Continuum medium
- Conservation equations (mass, momentum, energy) can be derived as averages of molecular properties
- Transport is given by averaging molecular fluxes. Under LTE Newton's, Fourier's and Fick's law are obtained



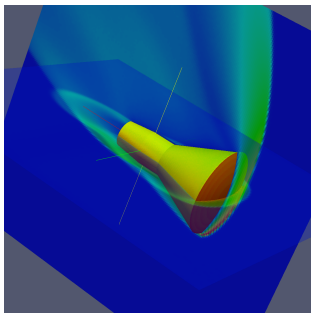
# Rarefied Gas Dynamics Regime

- High Mach number flight is more easily achieved in rarefied conditions (non-continuum).
- When non-continuum conditions prevail, flows are out of thermodynamic equilibrium.
  - not enough molecular collisions to maintain LTE.
- This flight regime results in high temperatures (more than 10,000K), chemically reacting, ionizing, radiating flows.

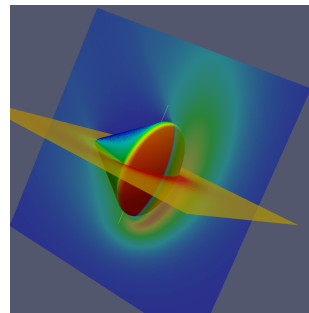


# Diffusing energy through re-entry

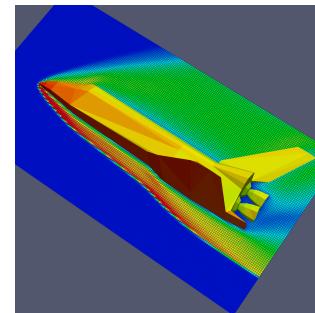
Gemini  
1961-1966



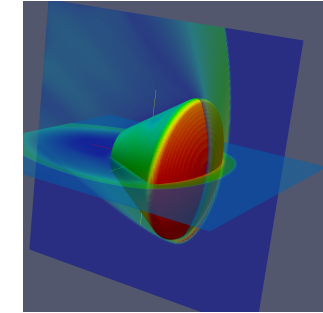
Apollo  
1963-1972



Space Shuttle  
1981-2011



Orion  
2014-?



- Atmospheric entry system must provide controlled dissipation of kinetic and potential energy of the vehicle.
- Dynamic and thermal loads must be kept within certain range

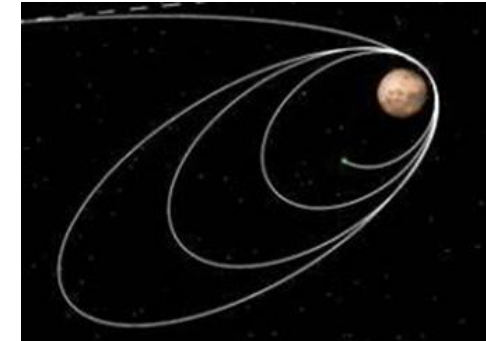
# The Mars Reconnaissance Orbiter mission

- Launch Date : August 12 2005
- Mars Orbit insertion : March 10 2006
- Final Orbit reached : August 30 2006



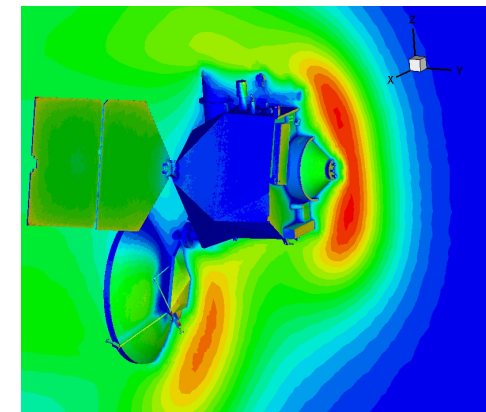
# Scope of MRO DSMC analysis

- Aerobraking was used to reduce fuel requirements during orbit placing maneuvers
- From a highly elliptic orbit the spacecraft was brought down to a near circular science orbit (255-320km)
- During the maneuvers the vehicle had to be aerodynamically stable and the heat load could not exceed maximum values

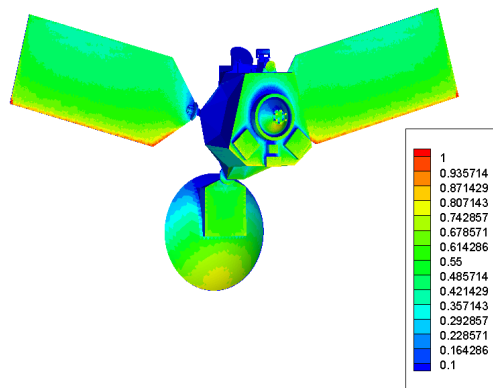
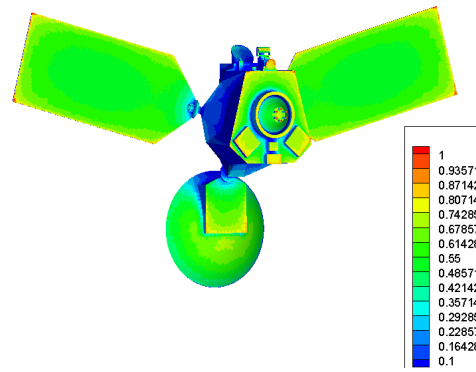
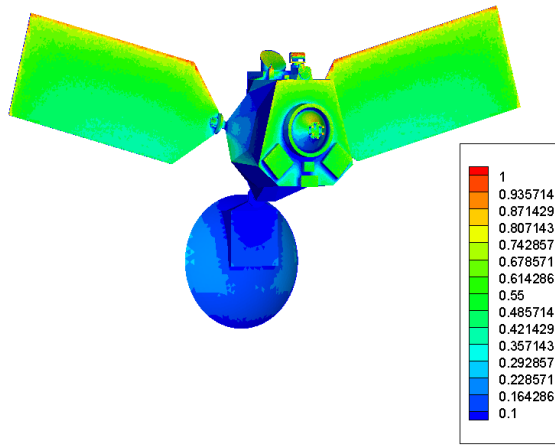


Scope of the following calculations :

- Define the heat transfer to the vehicle for a number of angles attack at nominal aerobraking altitude and velocity
- Define drag for a number of altitudes



# Heat flux for nominal aerobraking conditions



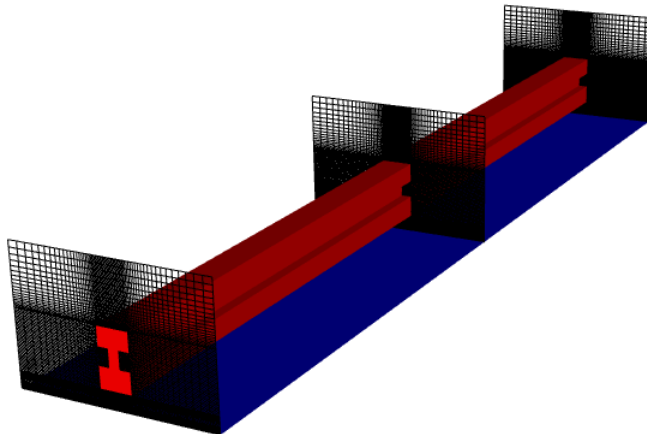
# Non-equilibrium effects

## Non-equilibrium effects:

- Non-Maxwell, Chapman-Enskog velocity distribution functions
- Non-linear transport properties
- Non-Boltzmann internal energy, no energy equipartition
- Non-Arrhenius chemical reactions
- Knudsen layers close to walls
- Can be caused by:
  - Reduced collisionality
  - Strong gradients even in near-continuum conditions

# Continuum but Non-equilibrium in MEMS Heated Microbeam Near Substrate

**Micro Electro Mechanical Systems (MEMS) reawakened interest in gas flow through long thin channels/tubes**



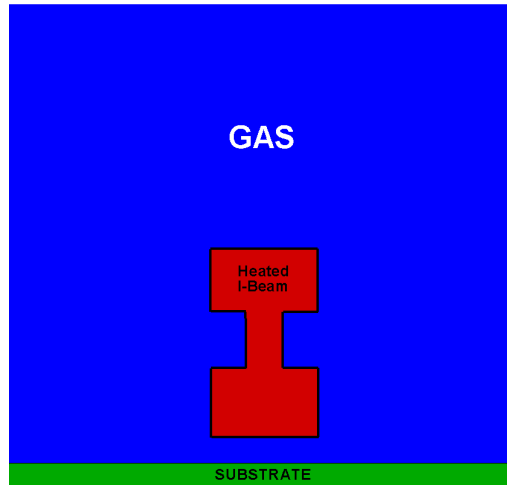
Solid regions: silicon

- Geometry: 2-micron gap
- Beam temperature: ~900 K
- Substrate temperature: ~300 K

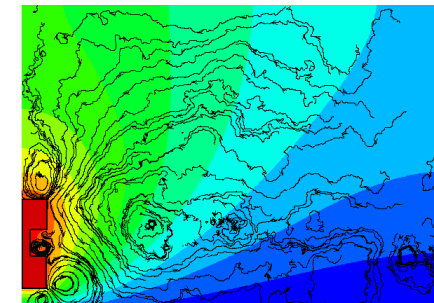
Gas region: nitrogen

- Pressure: atmospheric
- Initial temperature: ~300 K

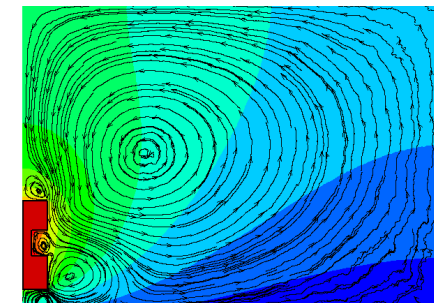
# Heated Microbeam makes Gas Move



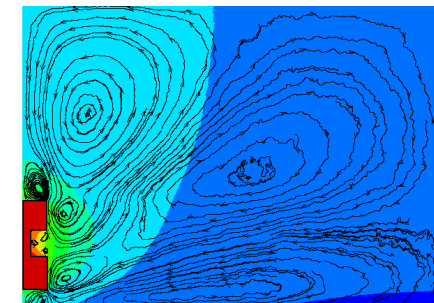
1 atm  
 $\sim 0.1$  m/s



0.1 atm  
 $\sim 2$  m/s



0.01 atm  
 $\sim 1$  m/s



## DSMC microbeam simulations

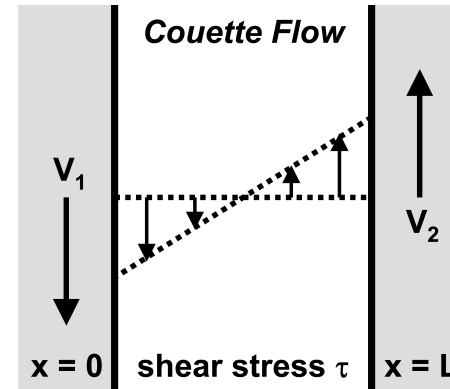
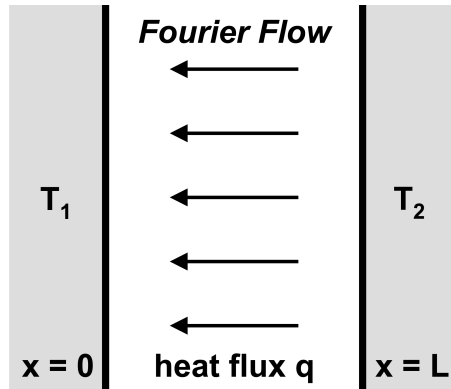
- Steady gas motion is induced by temperature differences  
*Not buoyancy, not transient*
- Noncontinuum effects cause motion  
*Not seen in NSSJ simulations*

# Fourier and Couette Flow



Joseph Fourier

$$q = -K \frac{\partial T}{\partial x}$$



Maurice Couette

$$\tau = \mu \frac{\partial v}{\partial x}$$

Investigate transport in gas between parallel plates

- Fourier flow: heat conduction in stationary gas
- Couette flow: momentum transport in isothermal shear flow

Apply DSMC to Fourier flow and Couette flow

- Heat flux, shear stress: one-dimensional, steady

Compare DSMC to analytical “normal solutions”

- Normal: outside Knudsen layers
- Solutions: Chapman-Enskog (CE), Moment-Hierarchy (MH)

Verify DSMC accuracy at arbitrary heat flux, shear stress

- Thermal conductivity, viscosity; velocity distribution

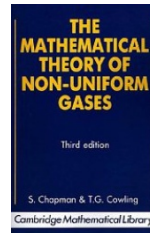
# Chapman-Enskog (CE) Theory



Sydney  
Chapman



David  
Enskog



$$\begin{aligned}
 f &= f^{(0)}(1 + \Phi^{(1)} + \Psi^{(1)}) & f^{(0)} &= (n/\pi^{3/2} c_m^3) \exp[-\tilde{c}^2] \\
 c_m &= \sqrt{2k_B T/m} & \tilde{\mathbf{c}} &= \mathbf{c}/c_m \quad \mathbf{c} = \mathbf{v} - \mathbf{u} \\
 \Phi^{(1)} &= -(8/5) \tilde{A}[\tilde{c}] \tilde{\mathbf{c}} \cdot \tilde{\mathbf{q}} & \Psi^{(1)} &= -2 \tilde{B}[\tilde{c}] (\tilde{\mathbf{c}} \circ \tilde{\mathbf{c}} : \tilde{\tau}) \\
 K &= -(5/4) k_B c_m^2 a_1 & \mu &= (1/2) m c_m^2 b_1 \\
 \tilde{A}[\tilde{c}] &= \sum_{k=1}^{\infty} (\textcolor{red}{a}_k / a_1) S_{3/2}^{(k)}[\tilde{c}^2] & \tilde{B}[\tilde{c}] &= \sum_{k=1}^{\infty} (\textcolor{red}{b}_k / b_1) S_{5/2}^{(k-1)}[\tilde{c}^2] \\
 C_p &= (5/2)(k_B/m) & \text{Pr} &= (2/3)(\textcolor{blue}{\mu}_{\infty}/\mu_1)(\textcolor{blue}{K}_1/K_{\infty})
 \end{aligned}$$

- Chapman and Enskog analyzed Boltzmann collision term
  - Perturbation expansion using Sonine polynomials
  - Near equilibrium, appropriate in continuum limit
- Determined velocity distribution and transport properties
  - Thermal conductivity  $K$ , viscosity  $\mu$ , mass self-diffusivity  $D$
  - Prandtl number  $\text{Pr}$  from “infinite-to-first” ratios  $K_{\infty}/K_1, \mu_{\infty}/\mu_1$
  - Distribution “shape”: Sonine polynomial coeffs.  $a_k/a_1, b_k/b_1$
  - Values for all Inverse-Power-Law (IPL) interactions
    - Maxwell and hard-sphere are special cases

# Extracting CE Parameters from DSMC

$$q = K_{\text{eff}} \left( \frac{\partial \textcolor{blue}{T}}{\partial x} \right)$$

$$\frac{a_k}{a_1} = \sum_{i=1}^k \left( \frac{(-1)^{i-1} k! (5/2)!}{(k-i)! i! (i+(3/2))!} \right) \left( \frac{\langle \tilde{c}^{2i} \tilde{c}_x \rangle}{\langle \tilde{c}^2 \tilde{c}_x \rangle} \right)$$

$$\tau = \mu_{\text{eff}} \left( \frac{\partial \textcolor{blue}{V}}{\partial x} \right)$$

$$\frac{b_k}{b_1} = \sum_{i=1}^k \left( \frac{(-1)^{i-1} (k-1)! (5/2)!}{(k-i)! (i-1)! (i+(3/2))!} \right) \left( \frac{\langle \tilde{c}^{2(i-1)} \tilde{c}_x \tilde{c}_y \rangle}{\langle \tilde{c}_x \tilde{c}_y \rangle} \right)$$

$$\tilde{\mathbf{c}} = \frac{\mathbf{v} - \textcolor{blue}{V}}{c_m}$$

$$c_m = \sqrt{\frac{2k_B \textcolor{blue}{T}}{m}}$$

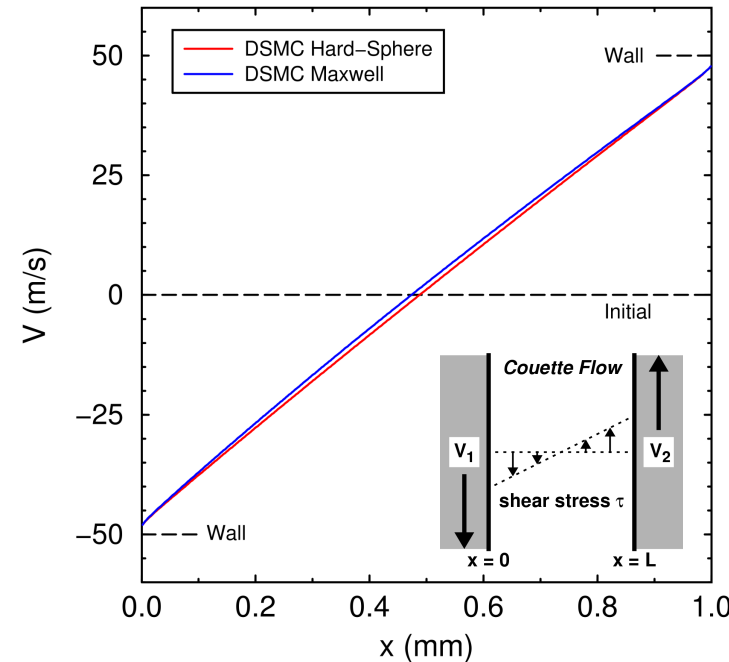
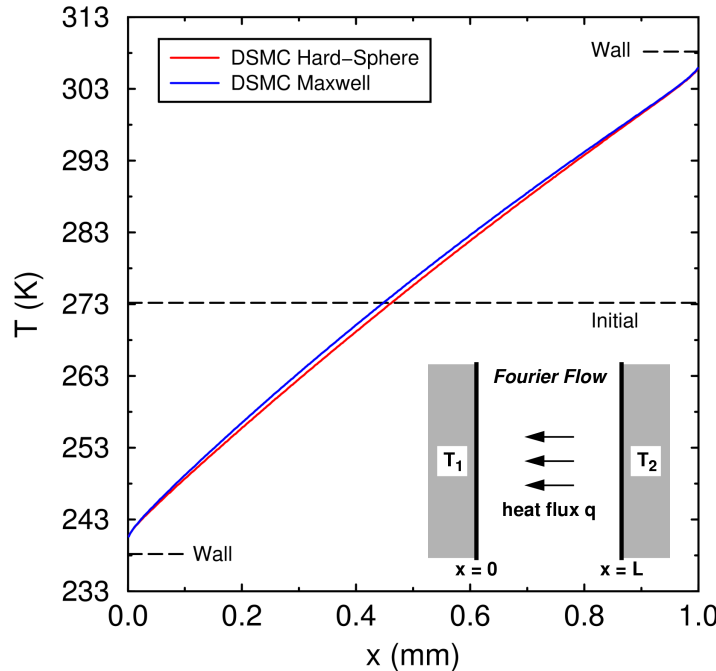
DSMC moments of velocity distribution function

- Temperature  $\textcolor{blue}{T}$ , velocity  $\textcolor{blue}{V}$
- Heat flux  $\textcolor{blue}{q}$ , shear stress  $\tau$
- Higher-order moments

DSMC values for VSS molecules (variable-soft-sphere)

- Thermal conductivity and viscosity:  $K_{\text{eff}}$  and  $\mu_{\text{eff}}$
- Sonine-polynomial coefficients:  $a_k/a_1$  and  $b_k/b_1$
- Applicable for arbitrary  $\text{Kn}_L$ ,  $\text{Kn}_q$ ,  $\text{Kn}_\tau$

# Temperature and Velocity Profiles

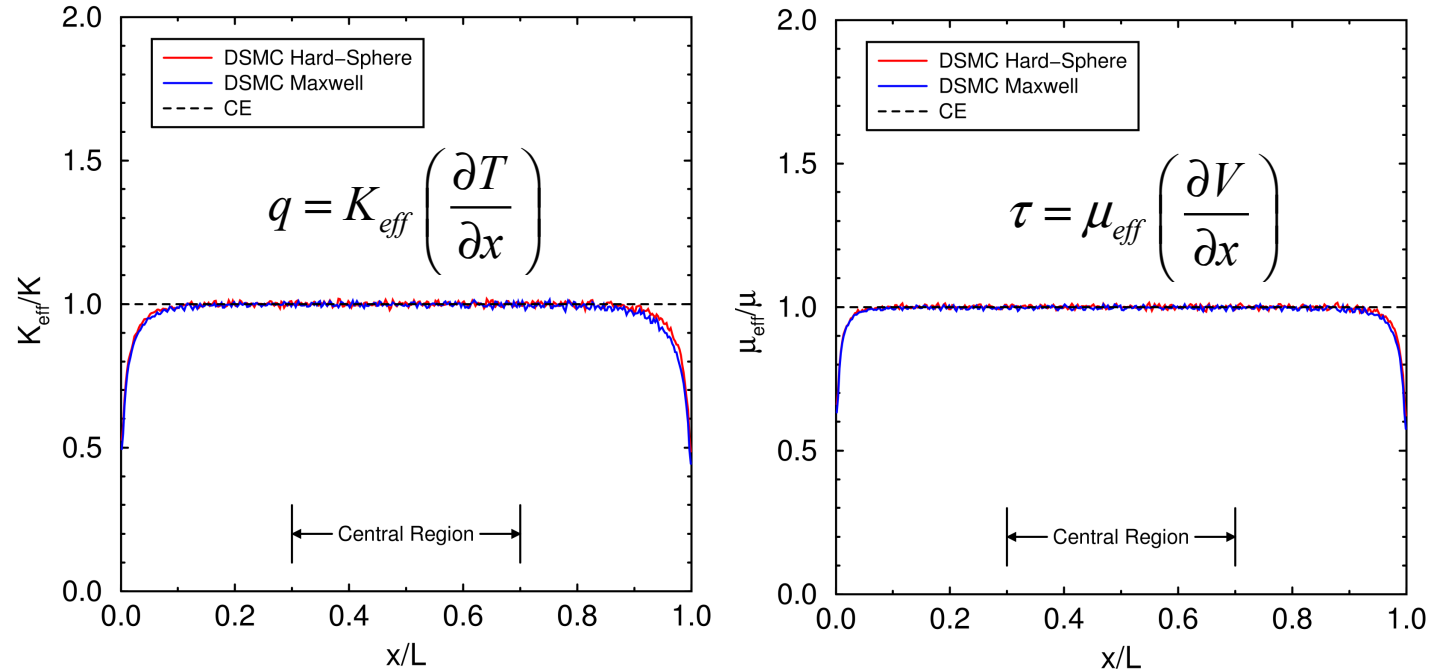


Low heat flux and shear stress:  $Kn_q = 0.006$ ,  $Kn_t = 0.003$

- Argon-like: initial  $T = 273.15$  K,  $p = 266.644$  Pa,  $l = 24$  mm
- Walls:  $L = 1$  mm =  $42l$ ,  $\Delta T = 70$  K,  $\Delta V = 100$  m/s
- $N_c = 120$ ,  $\Delta t = 7$  ns,  $\Delta x = 2.5$  mm,  $\sim 10^9$  samples/cell, 32 runs

Small velocity slips, temperature jumps, Knudsen layers

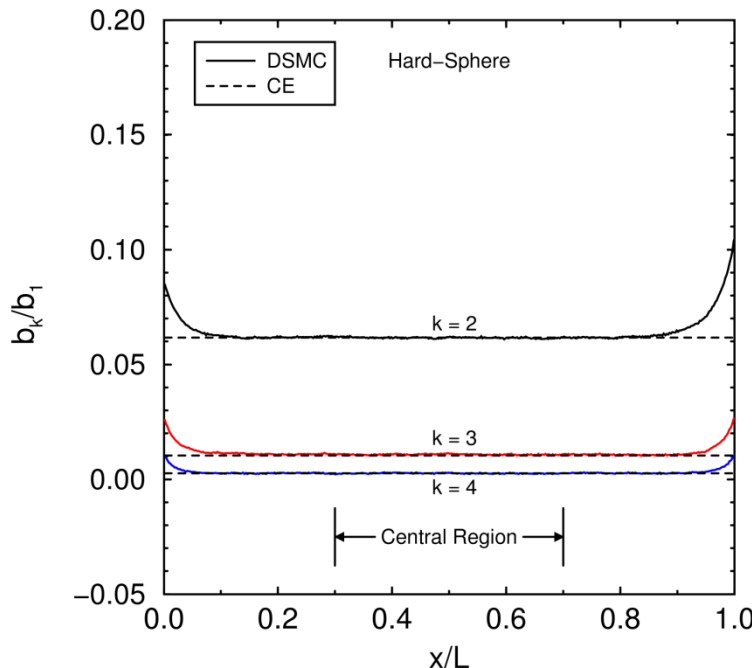
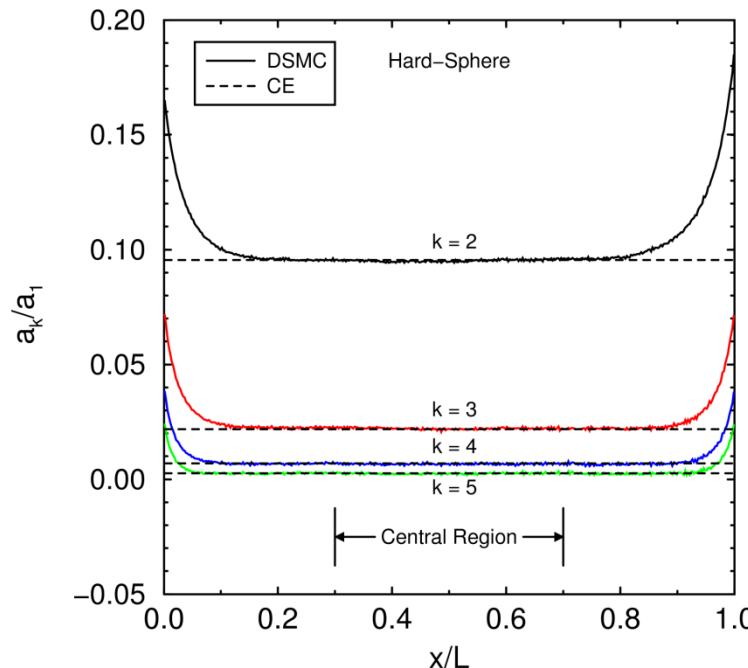
# DSMC Reproduces Infinite-Approximation Chapman-Enskog Transport Coefficients



Thermal conductivity (left) and viscosity (right) away from walls

- Maxwell and hard-sphere results bound most gases
- Agreement with Chapman-Enskog theory verifies DSMC

# DSMC Reproduces Infinite-Approximation Chapman-Enskog Velocity Distribution

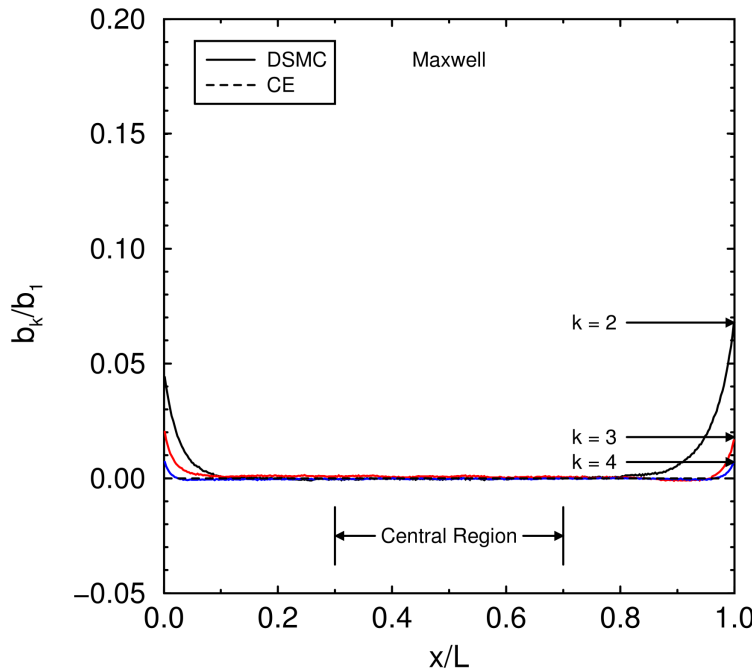
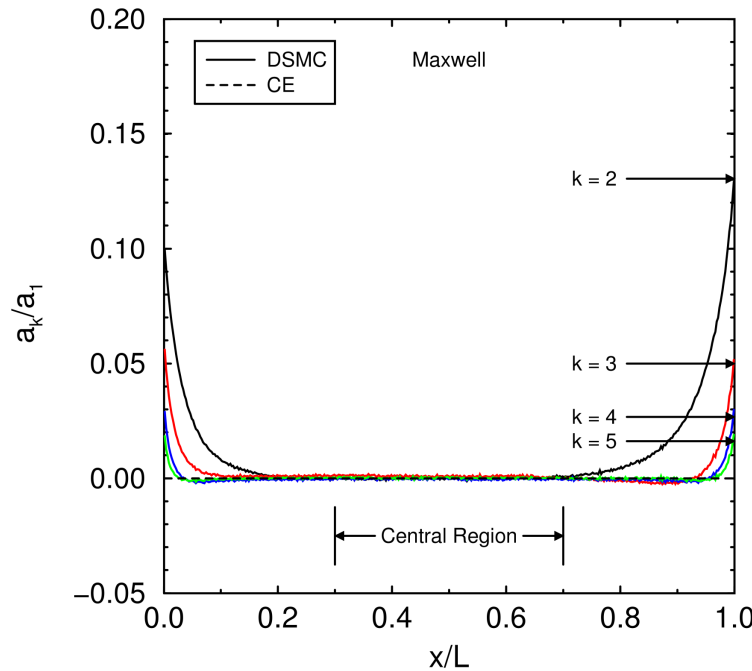


Sonine polynomial coefficients for temperature (left) & velocity (right) gradients

- Hard-sphere values are shown, other interactions have similar agreement
- Higher-order ( $k > 5$ ) coefficients (not shown) also have similar agreement

Gallis M. A., Torczynski J. R., Rader D. J., “Molecular Gas Dynamics Observations of Chapman-Enskog Behavior and Departures Therefrom in Nonequilibrium Gases”, *Physical Review E*, 69, 042201, 2004.

# Maxwell Sonine-Coefficient Profiles



DSMC and CE Maxwell coefficients  $a_k/a_1$  and  $b_k/b_1$

- Low heat flux, low shear stress:  $Kn_q = 0.006$ ,  $Kn_\tau = 0.003$
- Good agreement in central region: normal solution
- Knudsen layers easily observed:  $\sim 10\%$  of domain

# Moment-Hierarchy Method

$$M_{k_1 k_2 k_3} = \int \tilde{c}_x^{k_1} \tilde{c}_y^{k_2} \tilde{c}_z^{k_3} \tilde{f}[\tilde{\mathbf{c}}] d\tilde{\mathbf{c}} = \left\langle \tilde{c}_x^{k_1} \tilde{c}_y^{k_2} \tilde{c}_z^{k_3} \right\rangle$$

$$J_{k_1 k_2 k_3} = \text{Bilinear} \left[ \left\{ M_{k_1 k_2 k_3} \right\} \right]$$

$$K_{\text{eff}} / K = F_K[\text{Kn}_\tau] = 1 - \textcolor{blue}{c}_K \text{Kn}_\tau^2 + \mathcal{O}[\text{Kn}_\tau^4]$$

$$a_k / a_1 = (-1)^{k-1} \sum_{j=1}^{k-1} \textcolor{blue}{A}_{kj} \text{Kn}_q^{2j}$$

$$J_{k_1 k_2 k_3} = \int \tilde{c}_x^{k_1} \tilde{c}_y^{k_2} \tilde{c}_z^{k_3} J[\tilde{\mathbf{c}} | \tilde{f}, \tilde{f}] d\tilde{\mathbf{c}}$$

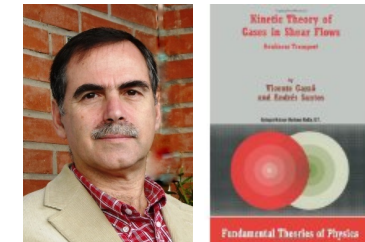
$$M_{k_1 k_2 k_3}[\text{Kn}_q, \text{Kn}_\tau] = \sum_{j=0}^{k_1+k_2+k_3-2} \textcolor{blue}{\mu}_{k_1 k_2 k_3}^{(j)}[\text{Kn}_\tau] \text{Kn}_q^j$$

$$\mu_{\text{eff}} / \mu = F_\mu[\text{Kn}_\tau] = 1 - \textcolor{blue}{c}_\mu \text{Kn}_\tau^2 + \mathcal{O}[\text{Kn}_\tau^4]$$

$$b_k / b_1 = (-1)^{k-1} \sum_{j=1}^{k-1} \textcolor{blue}{B}_{kj} \text{Kn}_q^{2j}$$

## Moment-Hierarchy (MH) normal solution

- Solve Boltzmann eqn. recursively for Maxwell molecules
- MH solution extends CE solution to finite  $\text{Kn}_q$  and  $\text{Kn}_\tau$
- Collision-term moments bilinear in distribution moments



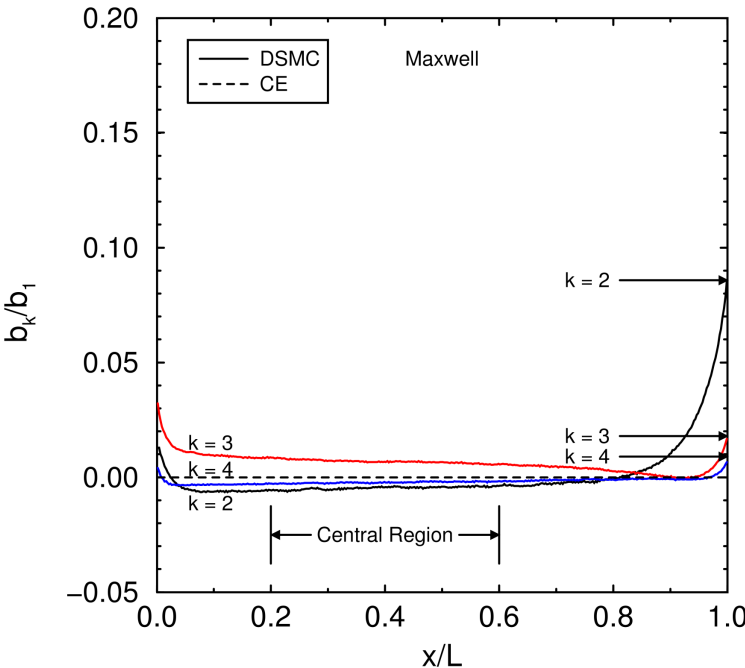
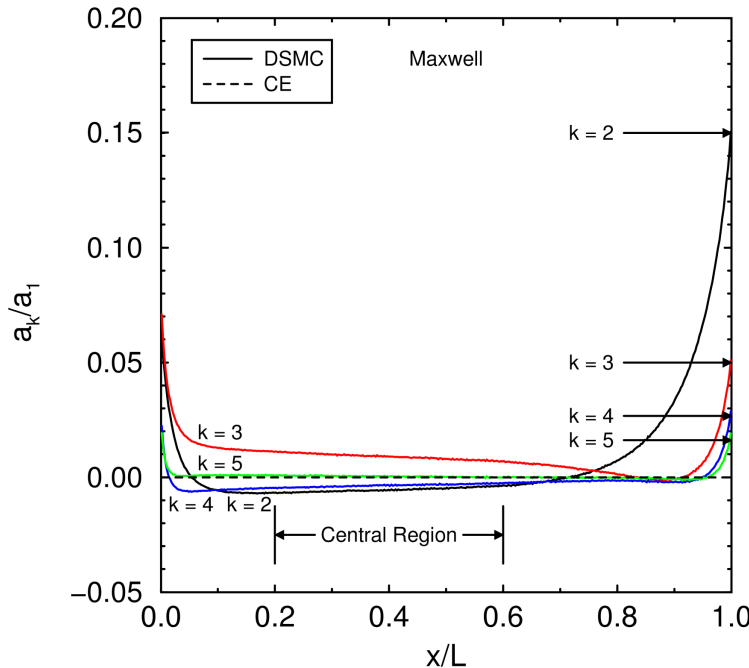
Andres Santos

## Compare MH and DSMC for Maxwell molecules

- Dependence of  $K$ ,  $m$ ,  $a_k/a_1$ ,  $b_k/b_1$  on  $\text{Kn}_q$  and  $\text{Kn}_\tau$

Gallis M. A., Torczynski J. R., Rader D. J., Tij M., Santos A., “Normal Solutions of the Boltzmann Equation for Highly Nonequilibrium Fourier and Couette Flow”, *Phys. Fluids*, 18, 017104, 2006.

# Maxwell Sonine-Coefficient Profiles



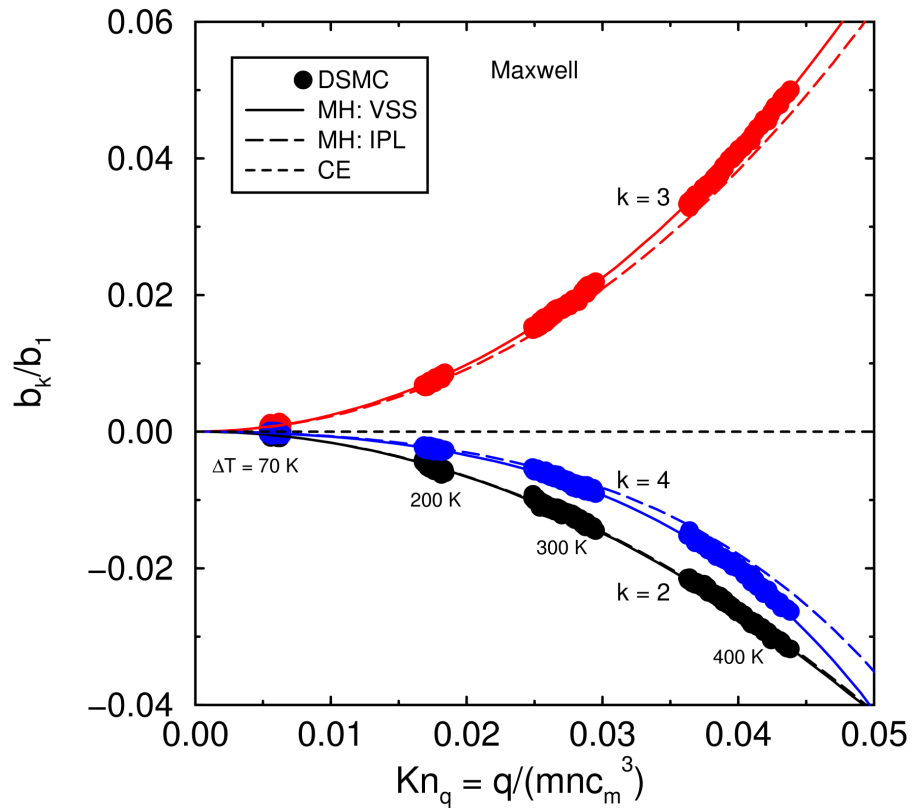
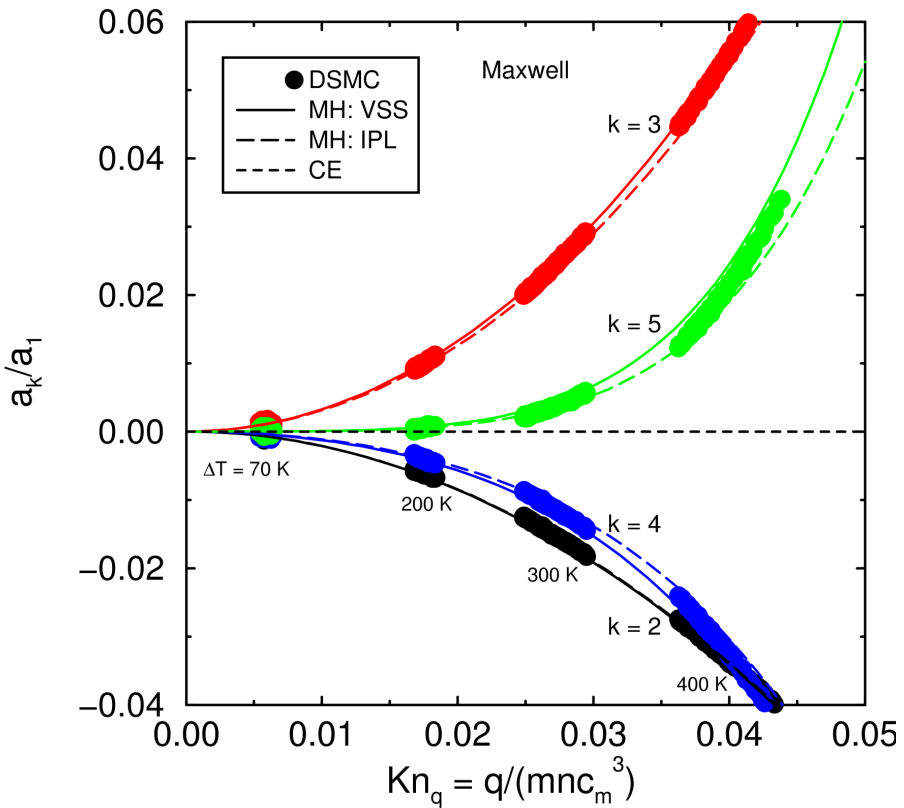
Finite heat flux, low shear stress:  $\text{Kn}_q \sim 0.017$ ,  $\text{Kn}_\tau = 0.003$

Maxwell Sonine-polynomial coefficients  $a_k/a_1$ ,  $b_k/b_1$

- CE and DSMC differ in central region:  $\text{Kn}_q$  not small
- Normal solution is nonuniform:  $\text{Kn}_q \sim T^{-1/2}$  and  $T = T[x]$

Plot DSMC values vs.  $\text{Kn}_q$  from central region

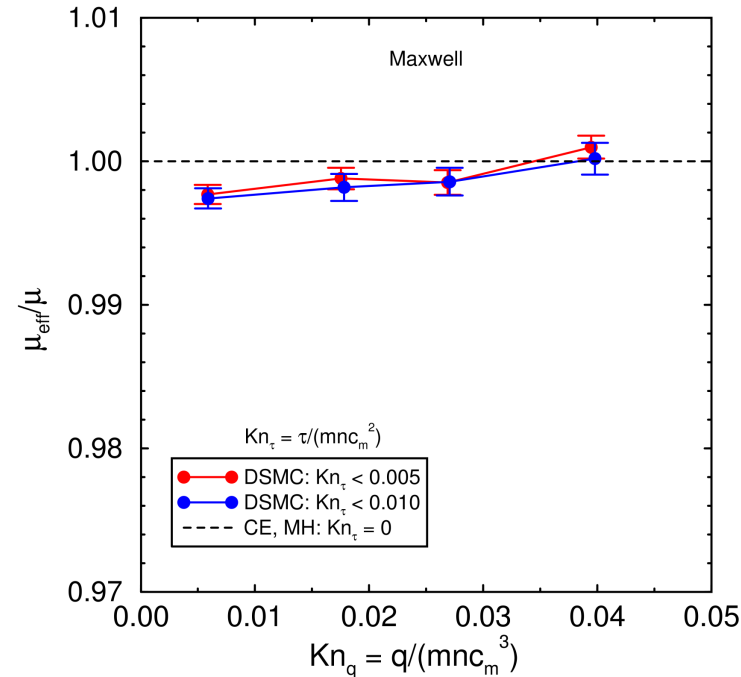
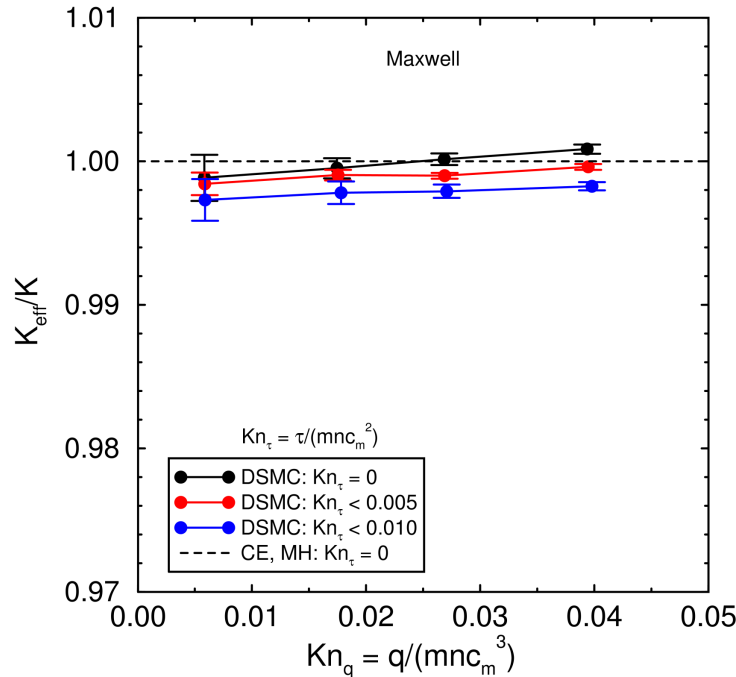
# Maxwell Normalized Sonine Coefficients



DSMC and MH Maxwell normal solutions for  $a_k/a_1$  and  $b_k/b_1$

- Four DSMC simulations:  $\Delta T = 70, 200, 300, 400 \text{ K}$
- MH: VSS-Maxwell (solid) and IPL-Maxwell (dashed) differ
- DSMC and MH VSS-Maxwell normal solutions agree

# Maxwell Normal Transport Coefficients

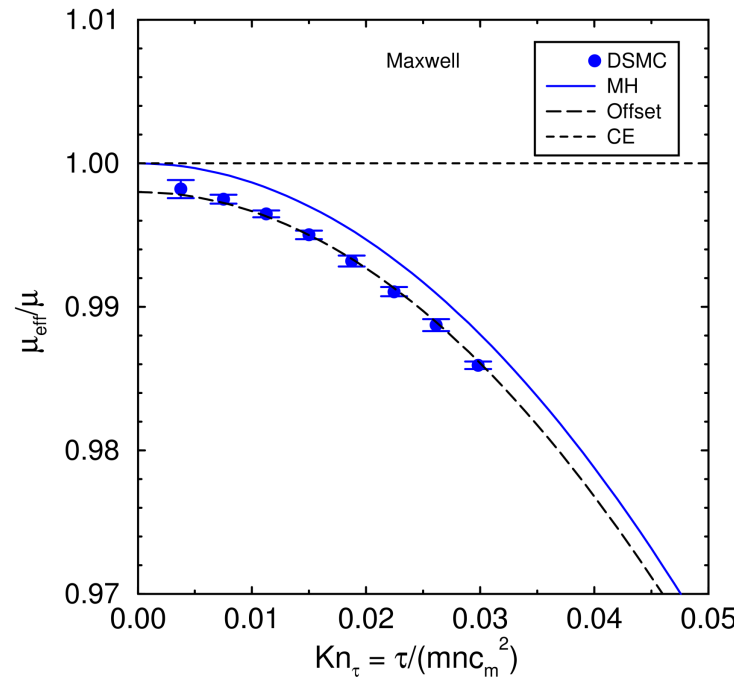
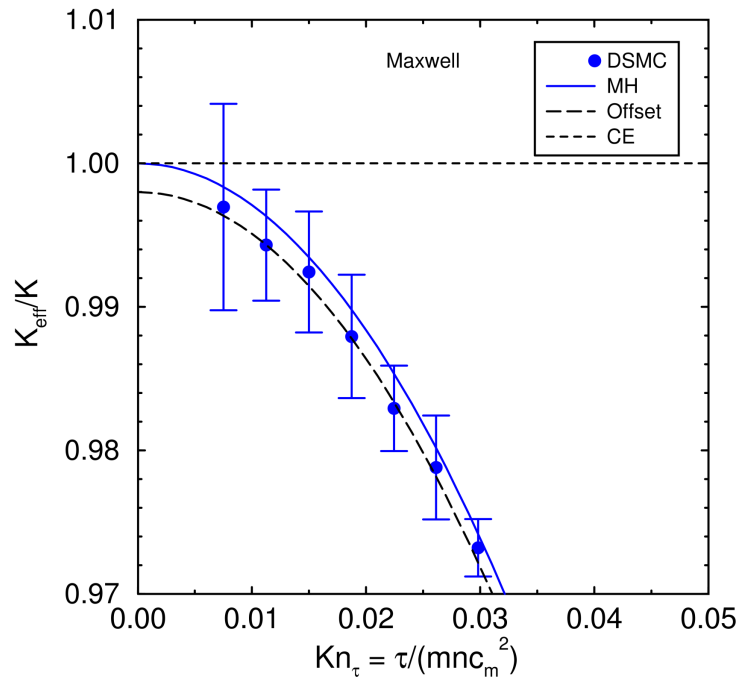


## DSMC and MH Maxwell normal solutions for K and $\mu$

- DSMC profiles look like low- $Kn_q$  profiles
- MH values for  $Kn_{\tau} = 0$  are independent of  $Kn_q$
- DSMC values approach MH values as  $Kn_{\tau} \rightarrow 0$
- DSMC values increase very slightly with  $Kn_q$

Agree to within DSMC discretization error

# Maxwell Normal Transport Coefficients

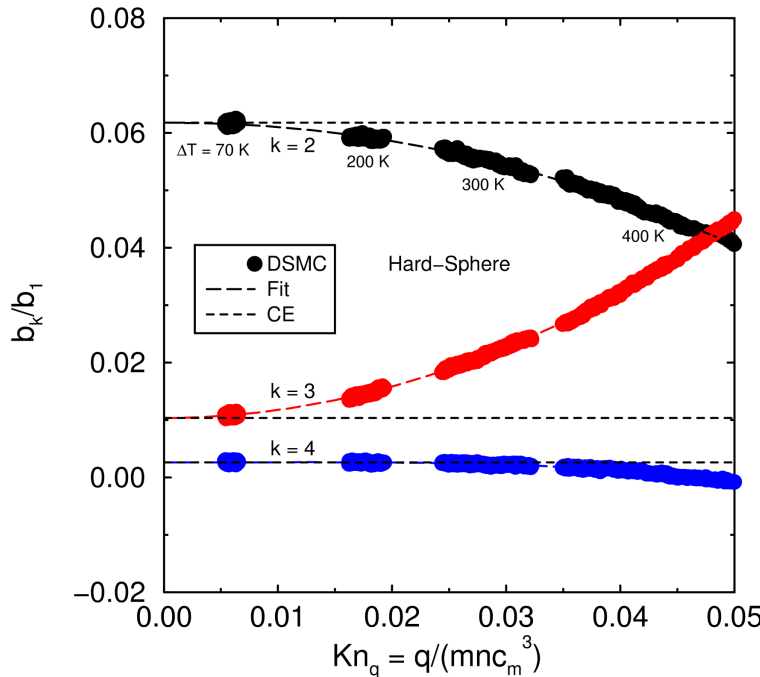
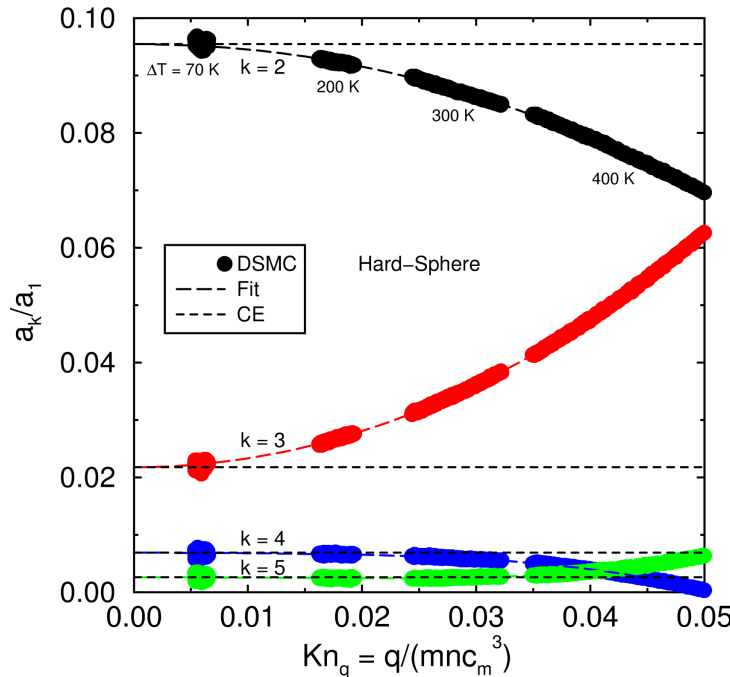


## DSMC and MH Maxwell normal solutions for K and m

- Finite  $Kn_t$  (shear stress), low  $Kn_q$  (heat flux)
- Eight DSMC simulations:  $\Delta V = 100, \dots, 800$  m/s
- Thermal conductivity from viscous heating, larger errors
- Offset MH by DSMC discretization error

Agree to within DSMC discretization error

# Hard-Sphere Sonine Coefficients

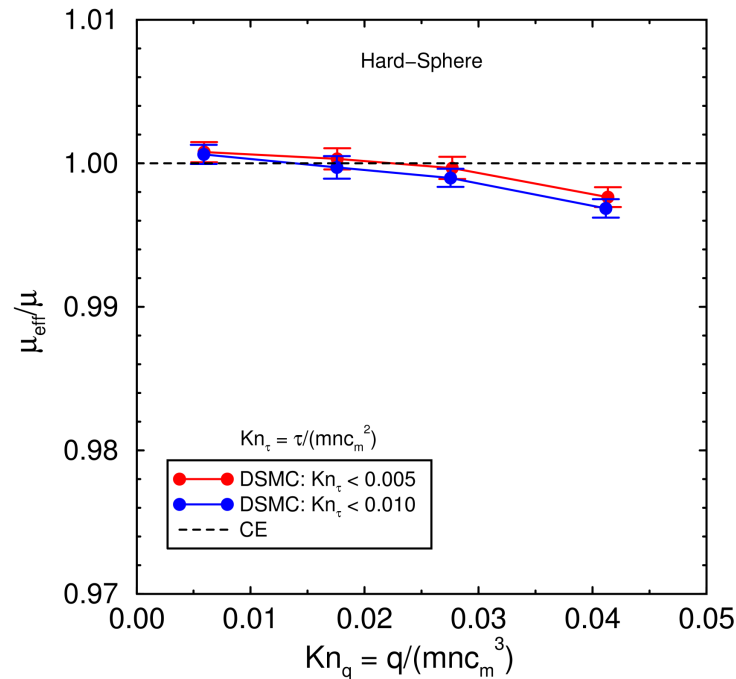
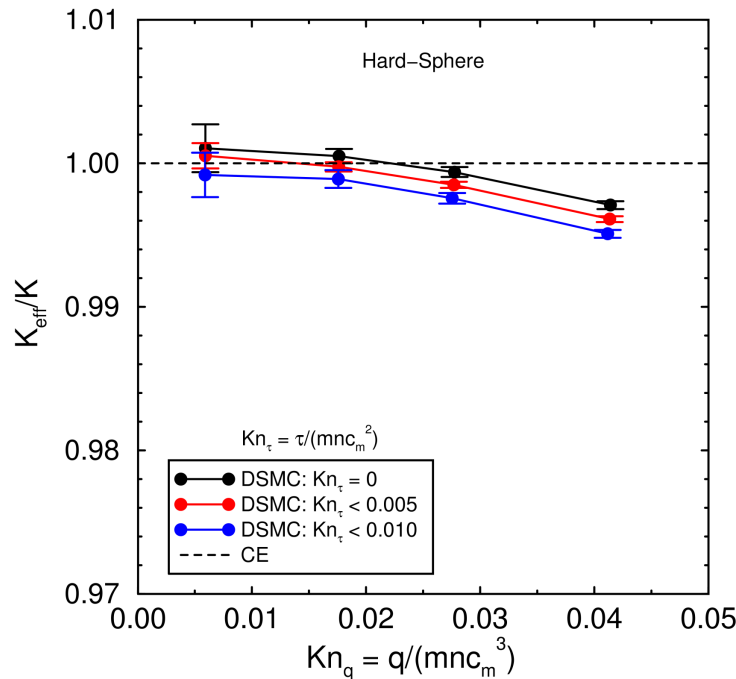


Hard-sphere normal solutions for  $a_k/a_1$  and  $b_k/b_1$

DSMC hard-sphere and VSS-Maxwell have same trends

- Four DSMC simulations at same conditions as Maxwell
- No exact results available: MH does not apply
- Even- $k$  terms decrease, odd- $k$  terms increase

# Hard-Sphere Normal Transport Coefficients

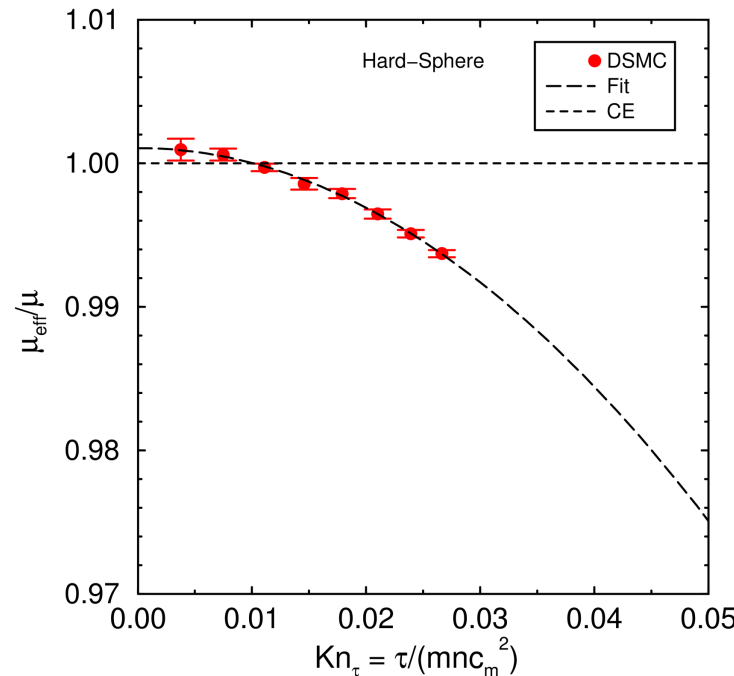
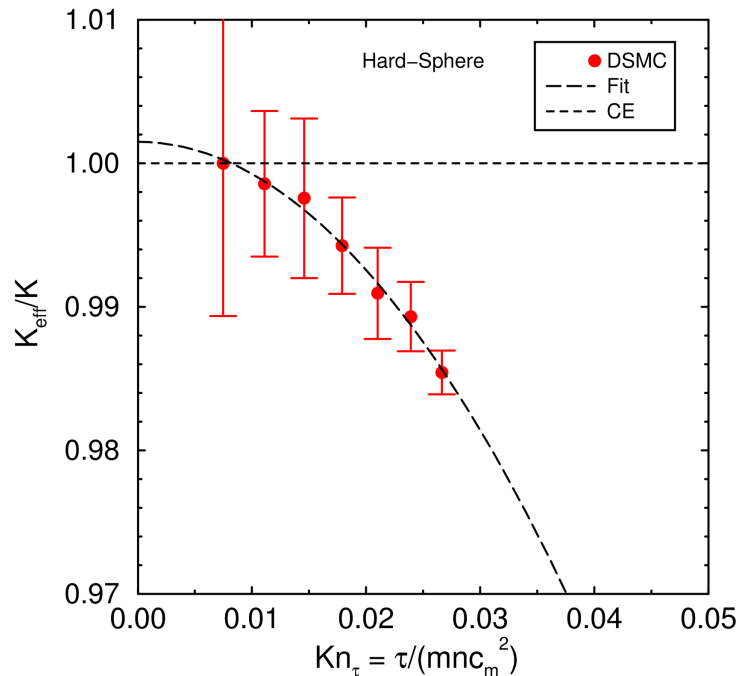


## DSMC hard-sphere normal solution for K and m

- No theoretical results available: MH does not apply
- DSMC values decrease slightly with  $Kn_q$
- Difference apparently greater than discretization error

Hard-sphere gas: “flux-insulating” and “flux-thinning”

# Hard-Sphere Normal Transport Coefficients



## DSMC hard-sphere normal solution for K and m

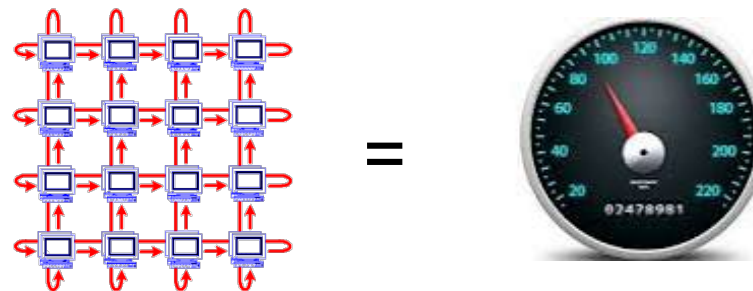
- Finite  $Kn_t$  (shear stress), low  $Kn_q$  (heat flux)
- No theoretical results available: MH does not apply
- DSMC values decrease with  $Kn_t$  (like Maxwell)

Hard-sphere gas: “shear-insulating” and “shear-thinning”

# Parallel Efficiency: The Unfair Advantage

- The advantages of DSMC come at a cost
- DSMC is **computationally efficient** but **computationally intense**
- Its successful application to real problems depends heavily on its parallel performance
- **1000x speedup** required for some problems of interest
- Monte Carlo methods usually have good parallel performance
  - The workload depends mainly on the simulators within a cell
  - Relatively less need to communicate information between cells
  - Trivial to parallelize in velocity space

The necessary speedup can be achieved without any loss of accuracy or convergence characteristics through parallel computing



# Top 5 Supercomputers (2014)

Rank	Site	System	Cores	Rmax (TFlop/s)	Rpeak (TFlop/s)
1	National Super Computer Center in Guangzhou	<b>Tianhe-2 (MilkyWay-2)</b> - TH-IVB-FEP Cluster, Intel Xeon E5-2692 12C 2.200GHz, TH Express-2, Intel Xeon Phi 31S1P	3,120,000	33,862.7	54,902.4
2	DOE/SC/Oak Ridge National Laboratory	<b>Titan</b> - Cray XK7 , Opteron 6274 16C 2.200GHz, Cray Gemini interconnect, NVIDIA K20x	560,640	17,590.0	27,112.5
3	DOE/NNSA/LLNL	<b>Sequoia</b> - BlueGene/Q, Power BQC 16C 1.60 GHz, Custom	1,572,864	17,173.2	20,132.7
4	RIKEN Advanced Institute for Computational Science (AICS)	<b>K computer</b> , SPARC64 VIIIfx 2.0GHz, Tofu interconnect	705,024	10,510.0	11,280.4
5	DOE/SC/Argonne National Laboratory	<b>Mira</b> - BlueGene/Q, Power BQC 16C 1.60GHz, Custom	786,432	8,586.6	10,066.3

# Programming for Next Generation and Exascale Machines

- Millions of nodes likely
- Reduced memory per node
- Parallelism within node:
  - Multi-core: 16 and growing
  - Many-core: Intel Xeon Phi, 240 threads
  - GPUs: NVIDIA/AMD, 1000 warps
- Example:
  - LLNL BG/Q: 96K nodes, 16 cores/node + 4 MPI tasks/core

Programming model: MPI + X

- Goal is to decouple the science code from the hardware details

Necessary elements

- Adaptive gridding
- In-situ visualization
- Efficient communications
- Load balancing



# Aiming for MPI+X via Kokkos

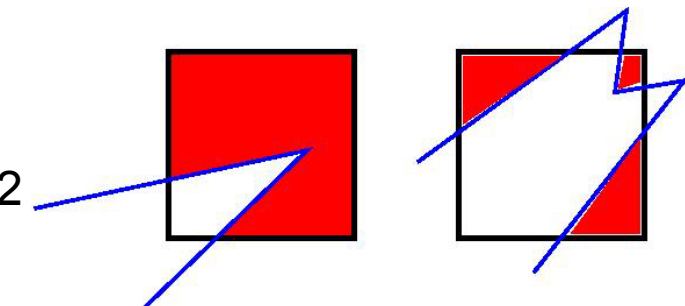
- What is Kokkos:
  - Programming model in development at Sandia
  - C++ template library
  - Open-source
  - Stand-alone
- Goal: write application kernels only once, and run them efficiently on a wide variety of hardware platforms
- Two major components:
  - Data access abstraction via Kokkos arrays optimal layout & access pattern for each device: GPU, Xeon Phi, etc.
  - Parallel dispatch of small chunks of work auto-mapped onto back-end languages: CUDA, OpenMP, etc.

# Developing an Exascale DSMC Code

**SPARTA** = Stochastic PArallel Rarefied-gas Time-accurate Analyzer

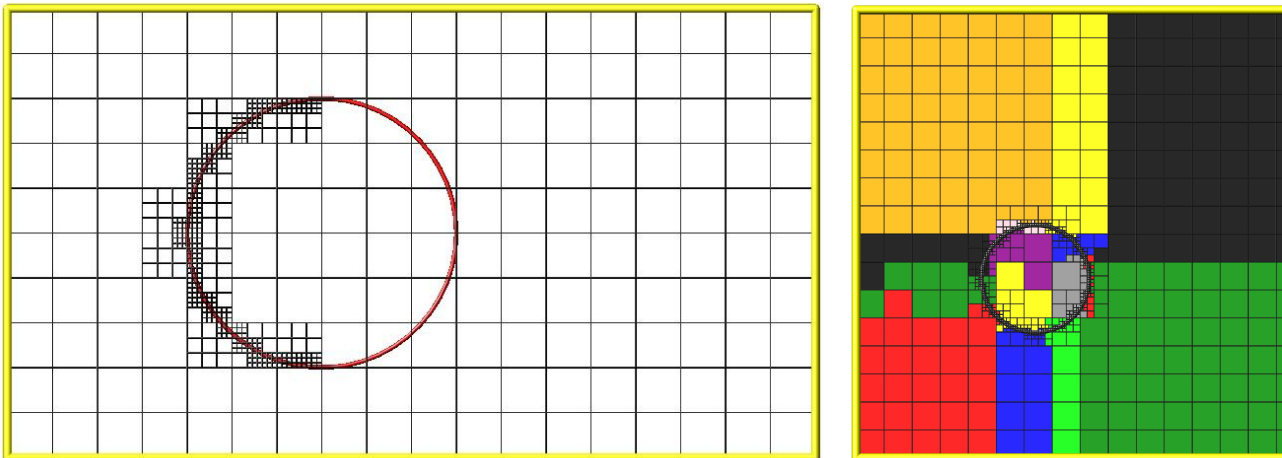
## General features

- 2D or 3D, serial or parallel
- Cartesian, hierarchical grid
  - Oct-tree (up to 16 levels in 64-bit cell ID)
  - Multilevel, general  $N \times M \times L$  instead of  $2 \times 2 \times 2$
- Triangulated surfaces cut/split the grid cells
  - 3D via Schwartzentuber algorithm
  - 2D via Weiler/Atherton algorithm
  - Formulated so can use as kernel in 3D algorithm
- C++, but really object-oriented C
  - Designed to be easy to extend
  - New collision/chemistry models, boundary conditions, etc.
- code available at <http://sparta.sandia.gov>



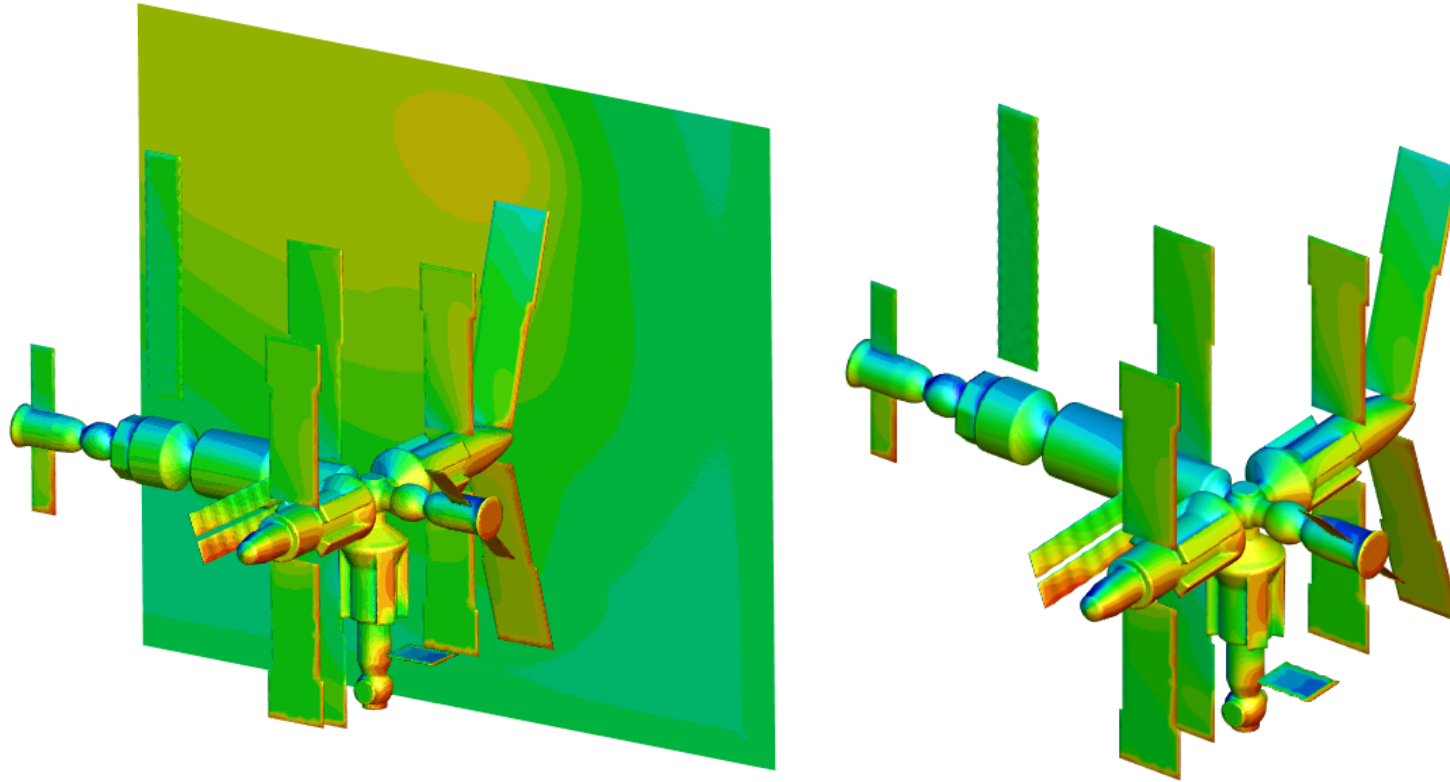
# Adaptive Gridding

- **Create/adapt grid in situ, rather than pre-process & read in**
- Examples: Generate around surface to user-specified resolution, adapt grid based on flow properties
- Algorithms should be efficient if they require only **local communications**



- Another setup task: label cells as outside/inside
- Simple if pre-processing, in situ easier for large problems

# Simulation of Complicated Shapes



Grid generation ( $10^7$  cells) completed in 0.3 seconds on 16 processors  
Geometry comprises multiple “water-tight” bodies

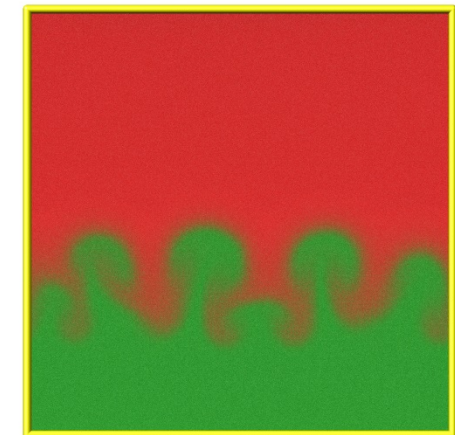
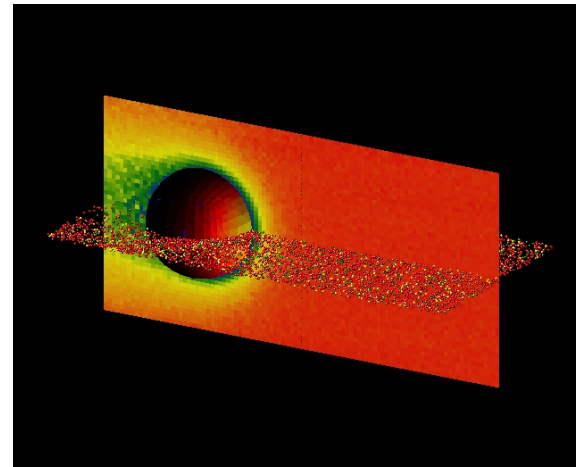
# In-Situ Visualization

Not a replacement for interactive viz, but ...  
Quite useful for **debugging** & quick analysis  
At end of simulation (or during), instant movie

Render a JPG snapshot every N time steps:

- Each processor starts with blank image (1024x1024)
- Processor draws its cells/surfaces/molecules with depth-per-pixel
- Merge pairs of images, keep the pixel in front, recurse
- Draw is parallel, merge is logarithmic (like MPI Allreduce)

Images are ray-traced quality



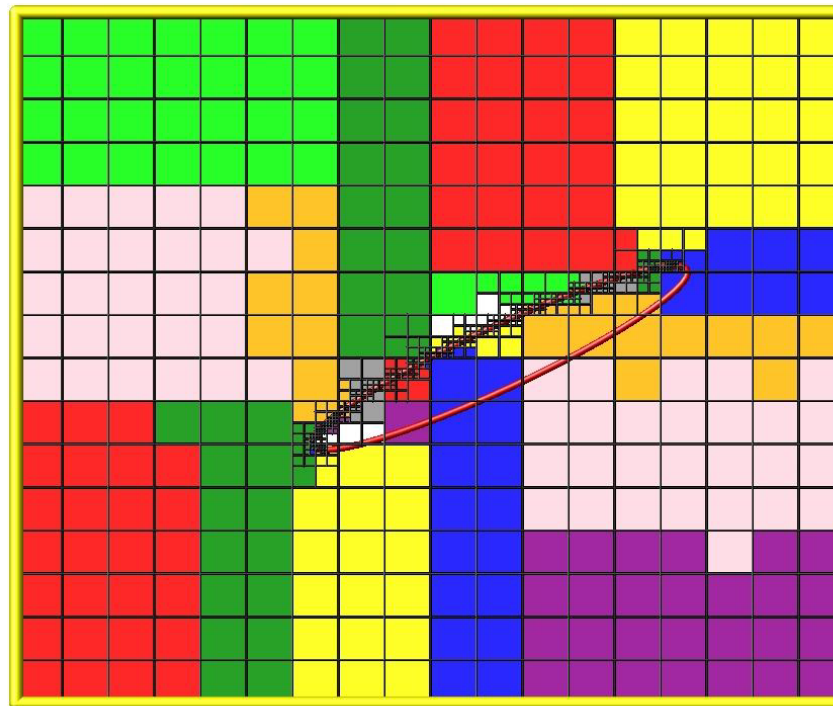
# Load Balancing

Balance across processors, **static or dynamic**

Granularity = grid cell with its molecules

Geometric method: recursive coordinate bisection (RCB)

**Weighted** by cell count or molecules or CPU



RCB is fast

Bigger cost is **data move**

Example:

1B cells on 1024 BG/Q nodes

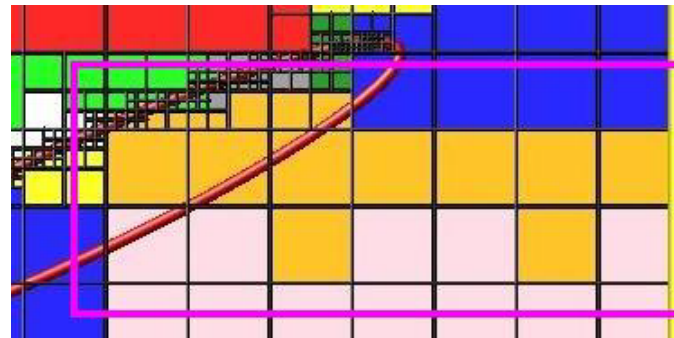
Worst case: move all cells

Balance time = 15 s:

(RCB=2, move=12, ghosts=1)

# Efficient Communication

- One processor = compact clump of cells via load balancing
  - Ghost region = nearby cells within **user-defined cutoff**
  - Store surface information for ghost cells to complete move



- Efficiently distributes grid information across processors
  - With sufficient cutoff, only **one communication per step**
  - Multiple passes if needed (or can bound molecule move)
- Communication with **modest count of neighbor processors**

# SPARTA Benchmarking

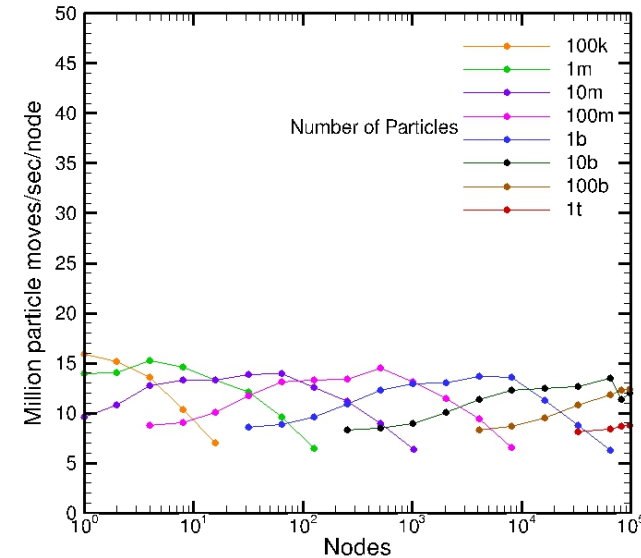
2 test cases:

- **Free-molecular**
  - Stress test for communication
  - 3D regular grid,  $10^4$ - $10^{11}$  (**0.1 trillion**) grid cells
  - 10 molecules/cell,  $10^5$ - $10^{12}$  (**1 trillion**) molecules
- **Collisional**
  - About 2x slower (sorting, collisions)
  - Same grid cell & molecule counts
- Effect of threading
  - **4 threads/core = 2x speed**

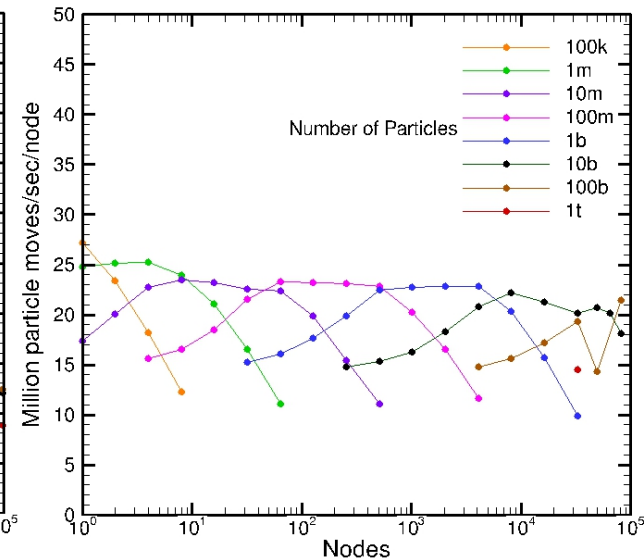


# SPARTA Benchmarking

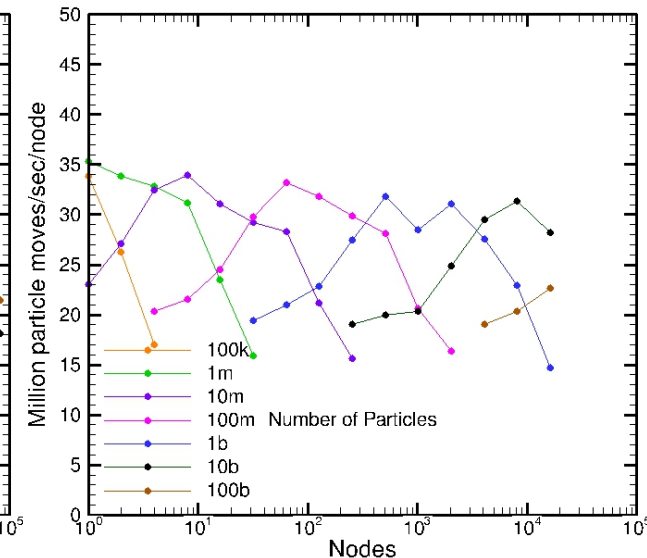
16 cores/node  
1 task/core



16 cores/node  
2 tasks/core



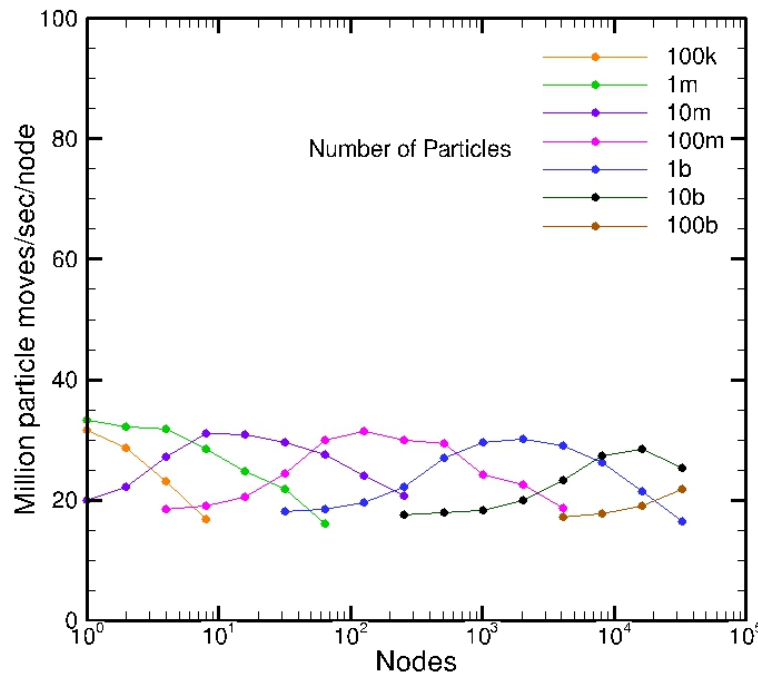
16 cores/node  
4 tasks/core



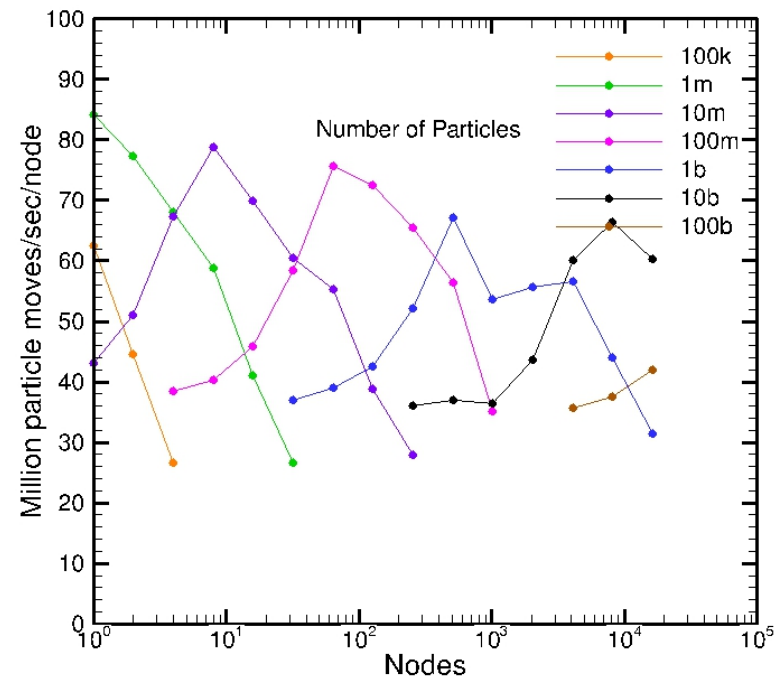
- Weak scaling indicates, 10% peak performance reduction from 1 to  $10^6$  cores
- 2 tasks/core gives 1.5x speedup, 4 tasks/core gives 2x speedup
- A total of **1 trillion simulators** can be simulated on **one third** of the BG/Q
- Maximum number of tasks is 2.6 million

# SPARTA Benchmarking (FM)

16 cores/node, 1 task/core



16 cores/node, **4** tasks/core



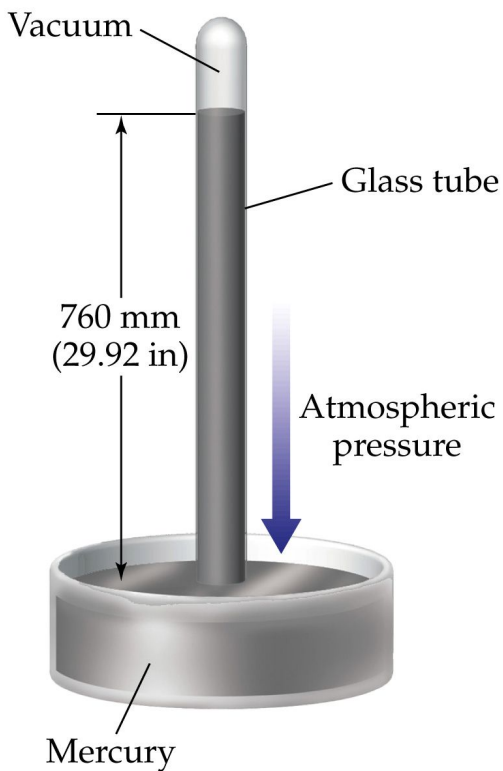
- Free-molecular (FM) calculations stress communications
- 2x speedup compared to collisional

# Torricelli's Mercury Barometer



Evangelista Torricelli

In 1643 pump makers attempted to raise water to a height of 12 meters or more, but found that 10 meters was the limit with suction pumps.

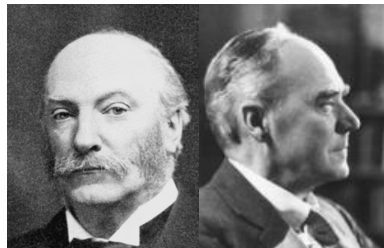


Torricelli employed a tube with mercury (14 times denser than water).

The mercury column stood at 76 cm indicating that **atmospheric pressure can support 10 m (=14x0.76) of water**



# The Rayleigh-Taylor Instability

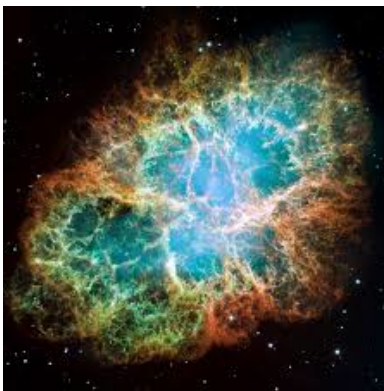


RTI is an interfacial instability that occurs when a high-density fluid is accelerated or supported by a low density one.



Small deviations from planarity (or sphericity) amplify with time and eventually led to mixing.

The growth of the instability is influenced by: viscosity, compressibility, three-dimensionality, density ratio



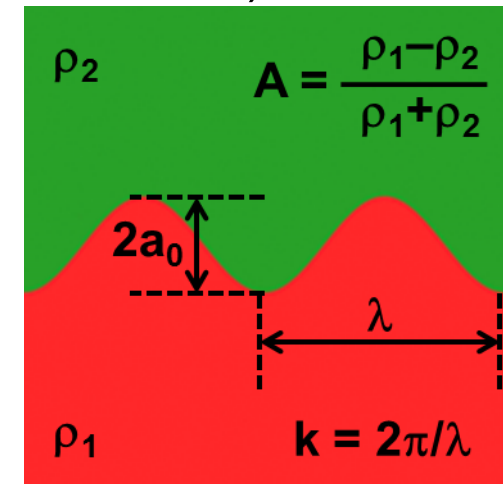
It is postulated that the failure to achieve ignition at NIF can be attributed to RMI.

Applications range from ICF (mm) to formation of supernova Remnants (light-years).

DSMC provides a molecular-level description of the hydrodynamic processes, that may be physically more realistic for large accelerations, chemically reacting flows

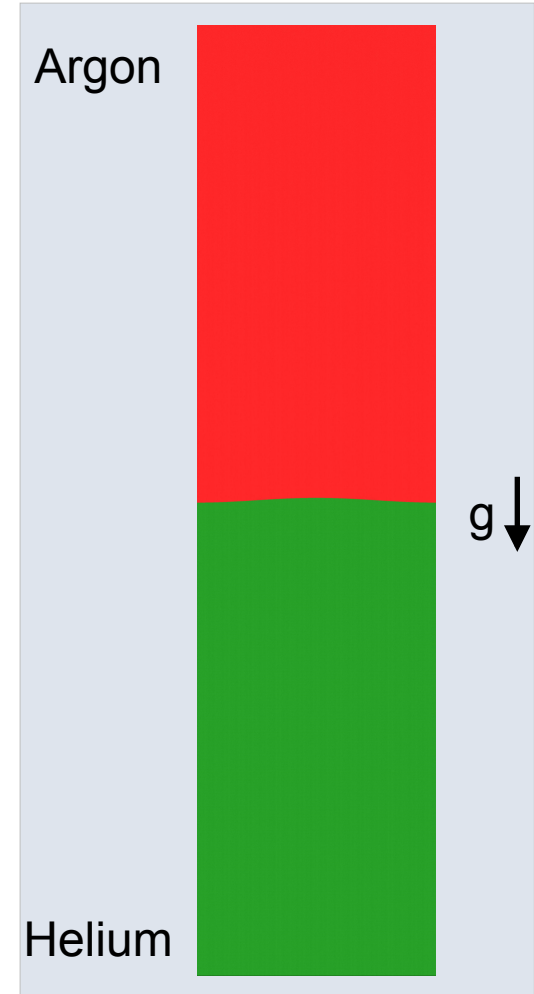
# DSMC for RTI

- DSMC provides a molecular-level description of the hydrodynamic processes, that may be physically more realistic for large accelerations, chemically reacting flows
- DSMC inherently accounts for transport properties
- The DSMC method offers the potential to identify the impact of molecular level effects (e.g. rotational and vibrational energy exchange, gas-phase chemical reactions, and gas-surface interactions) on hydrodynamic instabilities.
- Typical DSMC simulation characteristics:
  - Physical Domain: 1 mm x 4 mm (ICF-pellet size domain)
  - # Cells: 4,000,000,000
  - # Particles: 400,000,000,000
  - # Cores: 262,144-524,288

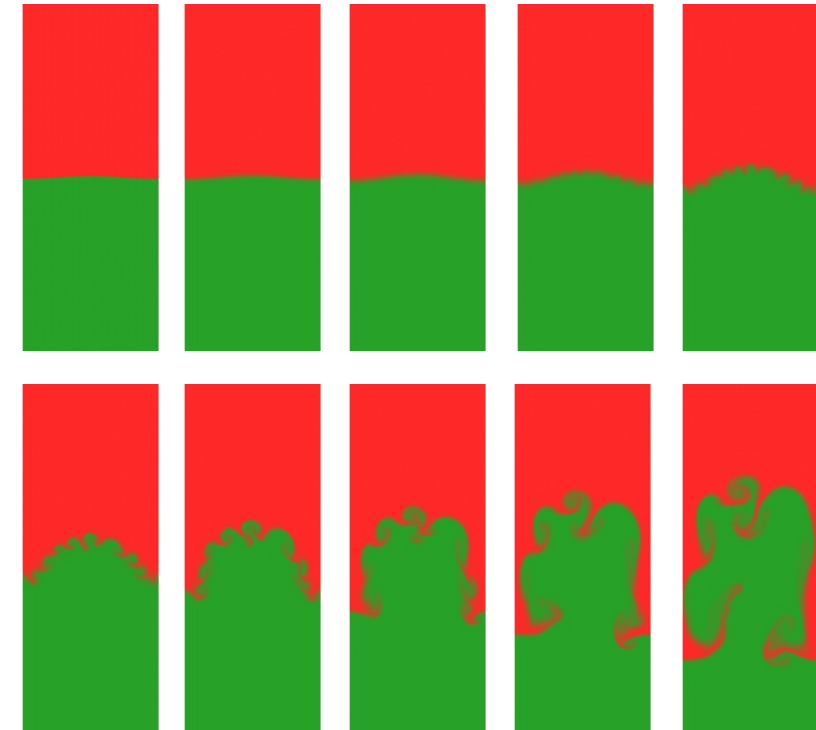
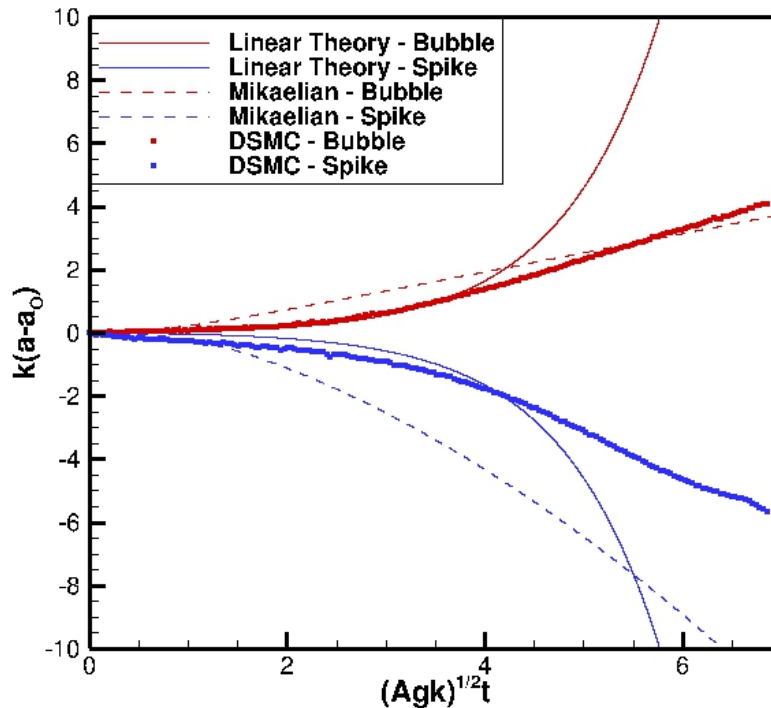


# DSMC Simulations of the Rayleigh-Taylor Instability in Gases

- The interface between Argon (red) and Helium (green) gases is slightly perturbed
- Acceleration of the system excites the RTI
  - Initially, thermal fluctuations / diffusion perturb the interface
  - The initial perturbation amplitude exponentially forming a bubble
  - A second growth stage occurs at the most unstable wavelength, also forming “bubbles” and “spikes”
  - Additional instabilities form breakup of the larger structures resulting in turbulent and chaotic mixing of the gases

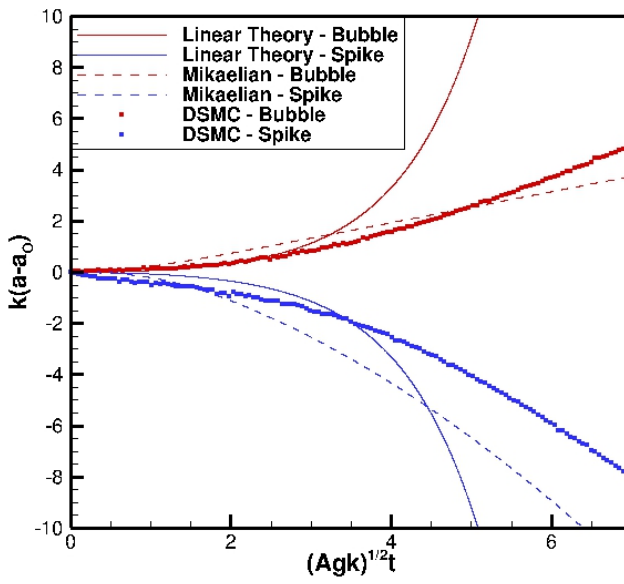
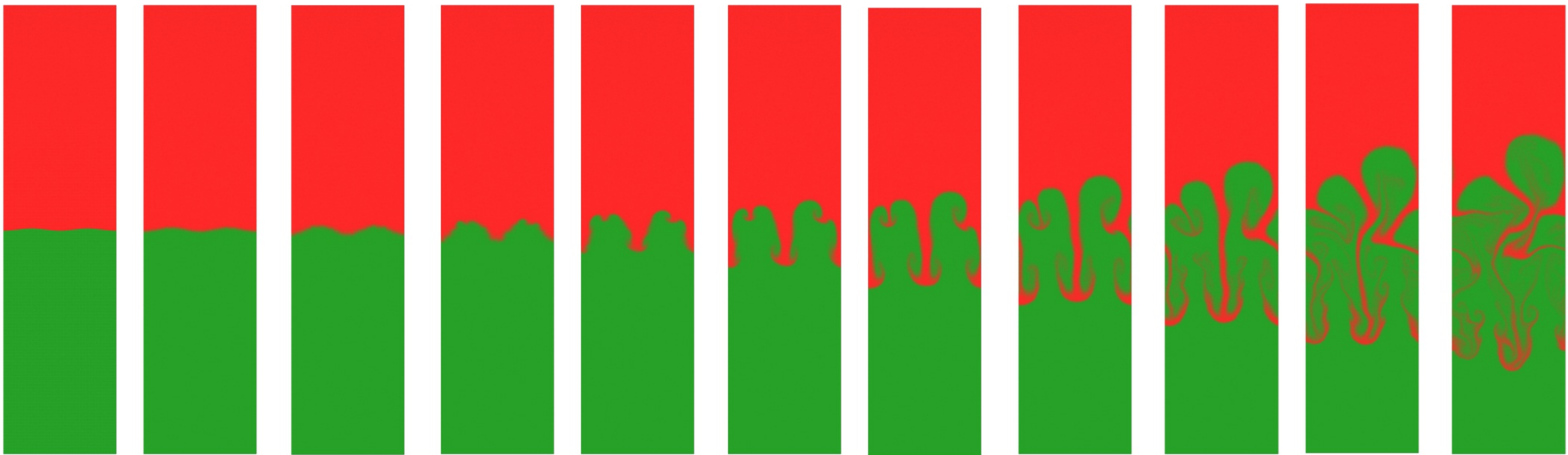


# Development of 0.001 m Wavelength Perturbation



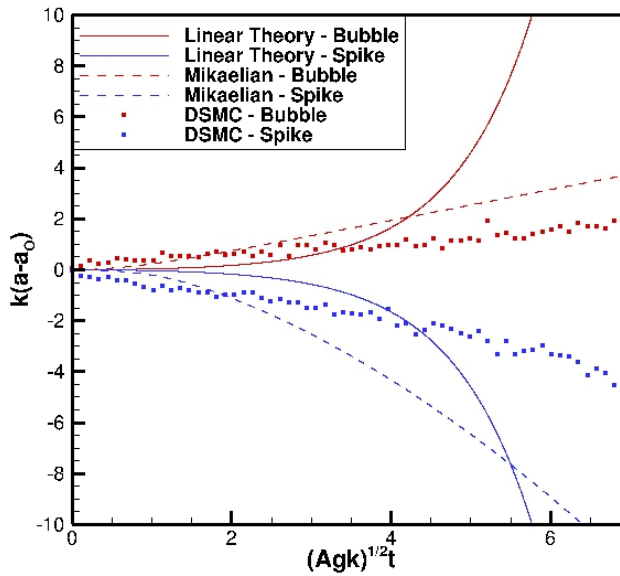
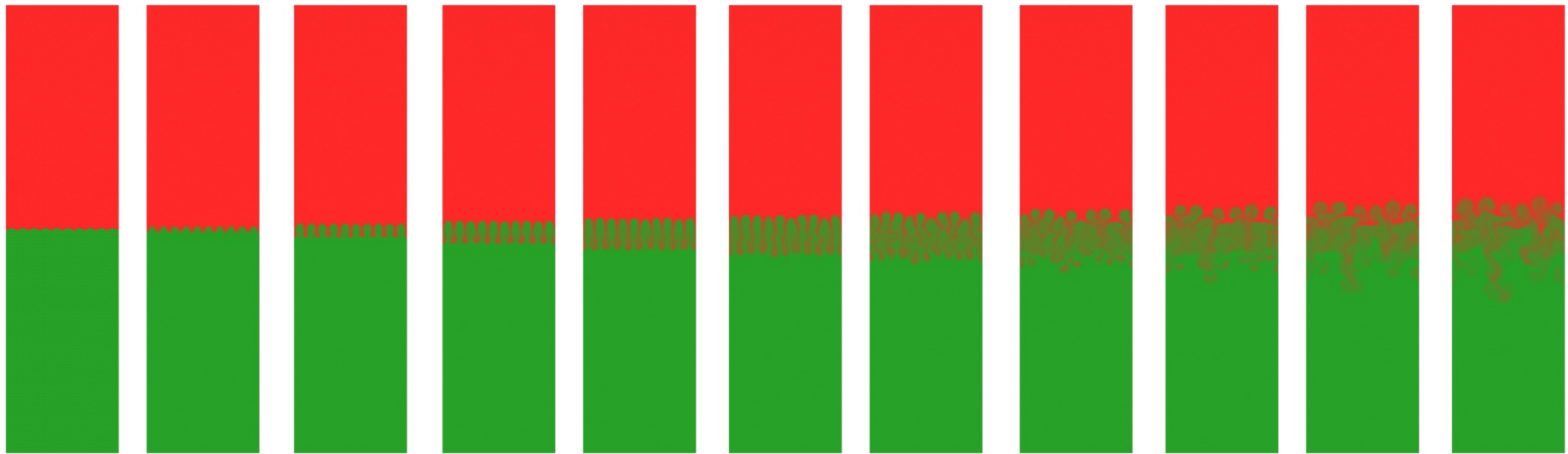
Initial perturbations of a small wavelength develop and grow exponentially. Appearance of larger structures as the smaller disturbances interact and combine. The structures themselves develop instabilities like the Kelvin-Helmholtz instability, which eventually break up the structures, resulting in turbulent and chaotic mixing of the fluids.

# Development of 0.0005m Amplitude Perturbation



Reasonable agreement with linear theory for small amplitudes  
Qualitative agreement with Mikaelian's model for Linear and Non-Linear regime

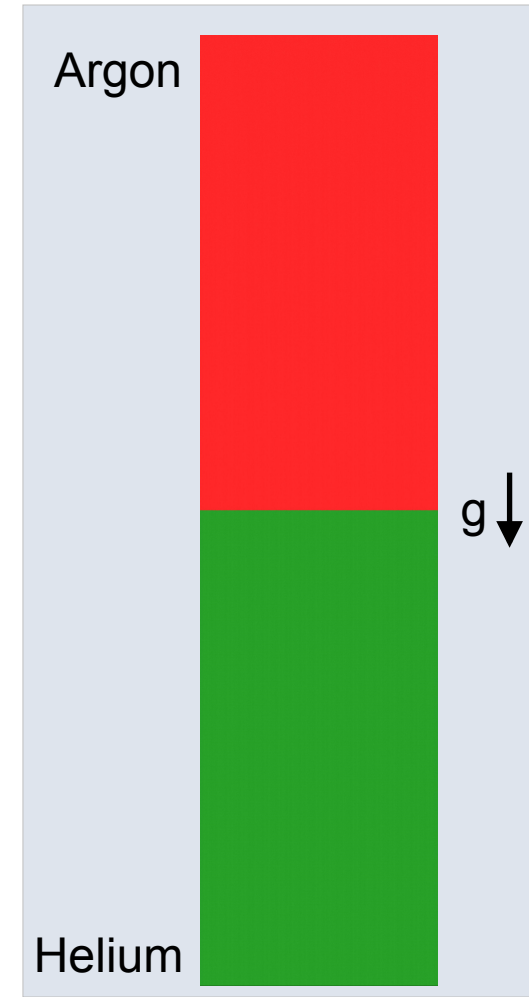
# Development of 0.0001m Amplitude Perturbation



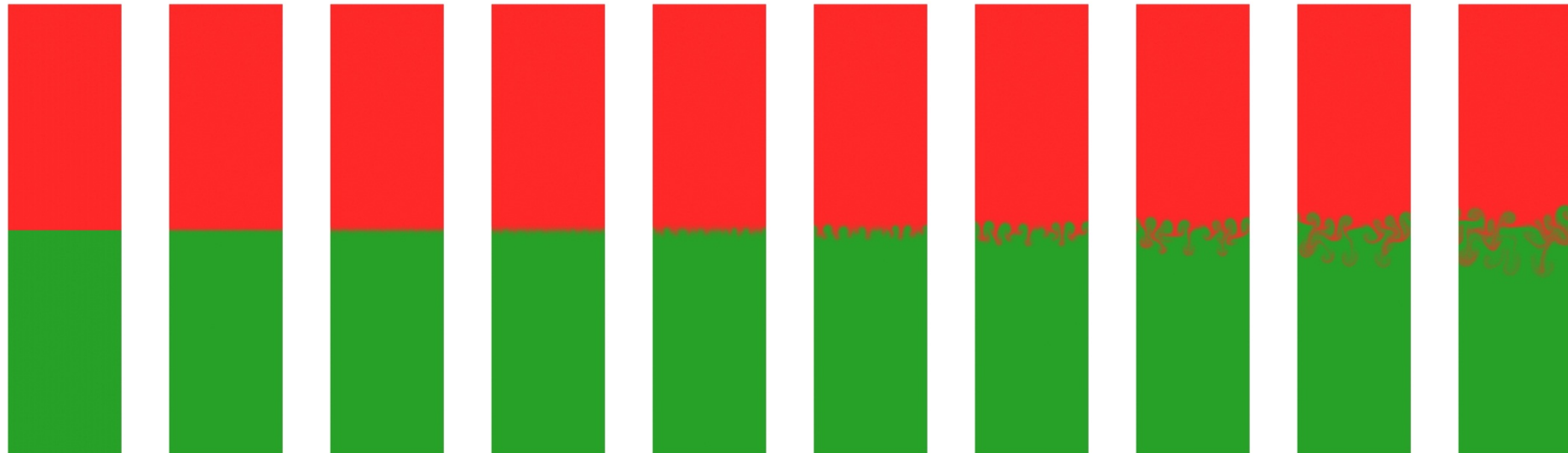
Reasonable agreement with linear theory for small amplitudes  
Qualitative agreement with Mikaelian's model for Linear and Non-Linear regime

# RTI from an Initially Molecularly Flat Interface

- The interface between Argon (red) and Helium (green) gases is **initially flat**
- Acceleration of the system excites the RTI
  - Initially, thermal fluctuations / diffusion perturb the interface
  - The amplitude of these perturbations grows exponentially
  - A second growth stage occurs during which the gases penetrate each other differently, forming “bubbles” and “spikes”
  - Finally, additional instabilities form breakup of the larger structures resulting in turbulent and chaotic mixing of the gases



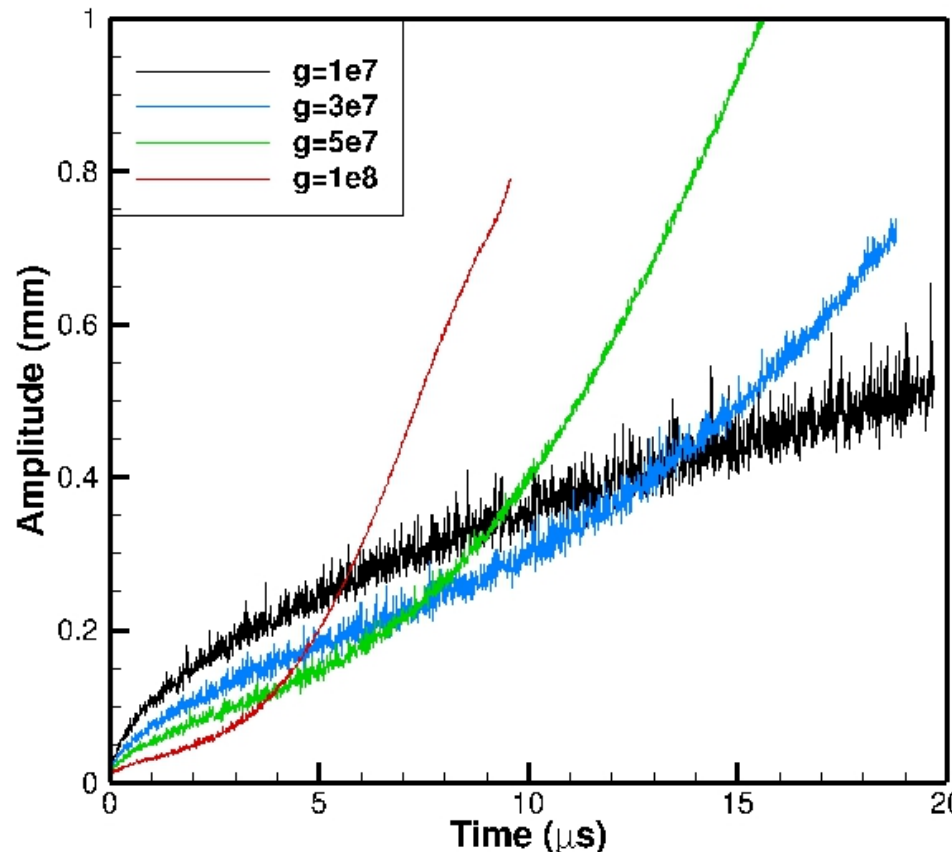
# RTI from an Initially Flat Interface



Images progress at 10,000 time step increments

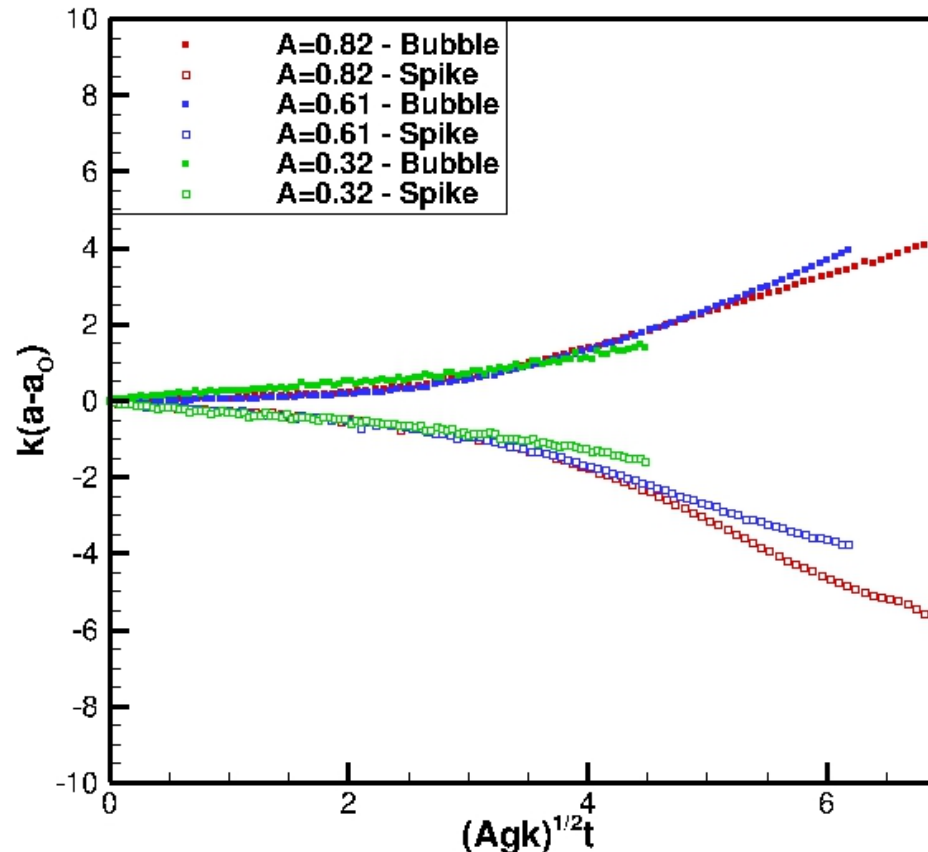
The number of bubbles and spikes correspond to the most unstable wavelength

# RTI: Effect of Gravity



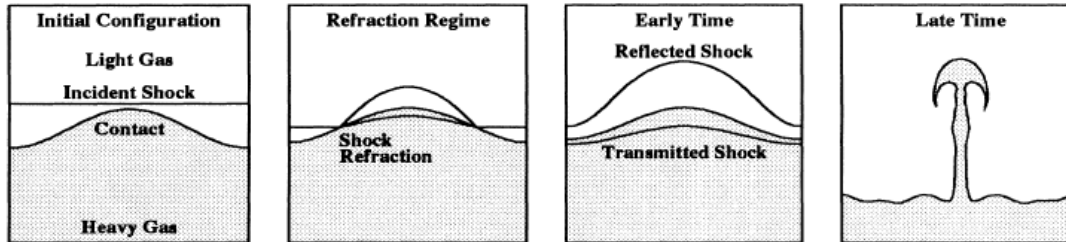
Initially the interface grows due to diffusion followed by exponential and non-linear growth

# RTI. Effect of Atwood Number

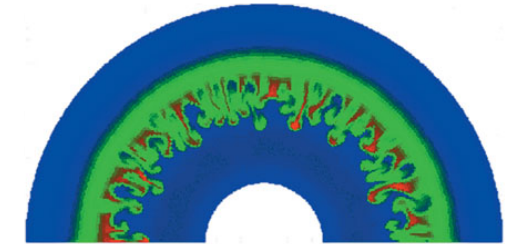


The effect of Atwood number becomes significant in the non-linear region

# Richtmyer-Meshkov Instability (RMI)



Grove et al., Phys. Rev. Lett., 71(21), 3473 (1993).

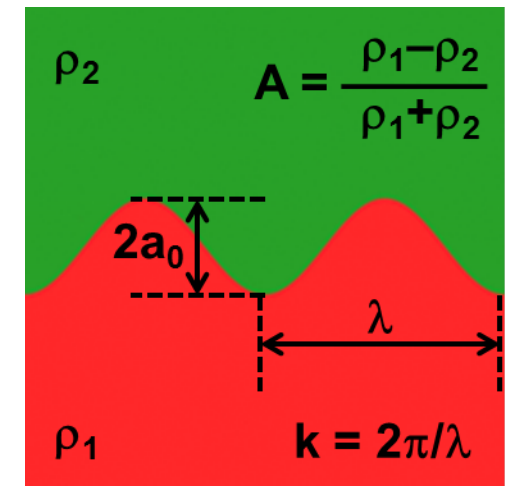


ICF target compression

RMI applications include stellar evolution, inertial confinement fusion, shock-flame interaction

RMI combines multiple fluid-flow phenomena

- Shock transmission and reflection
- Hydrodynamic instabilities
- Linear and nonlinear growth
- Diffusion and turbulent mixing
- Compressibility effects
- Chemical reactions



RMI basic geometry

## *Simulate RMI using molecular gas dynamics*

- Physical conditions that can be achieved
- Computational software & hardware needed

# RMI in Air/SF<sub>6</sub> Mixture: Mach 1.4 Shock

## Physical situation

- Gases: pairs of helium, neon, argon, xenon, air, SF<sub>6</sub>
- STP conditions: both gases at 1 atm and 0 °C
- Two-dimensional domain: 0.1 mm × 0.4 mm
- Wavelength, initial amplitude: 0.05 mm, 0.01-0.1 mm

## Numerical parameters

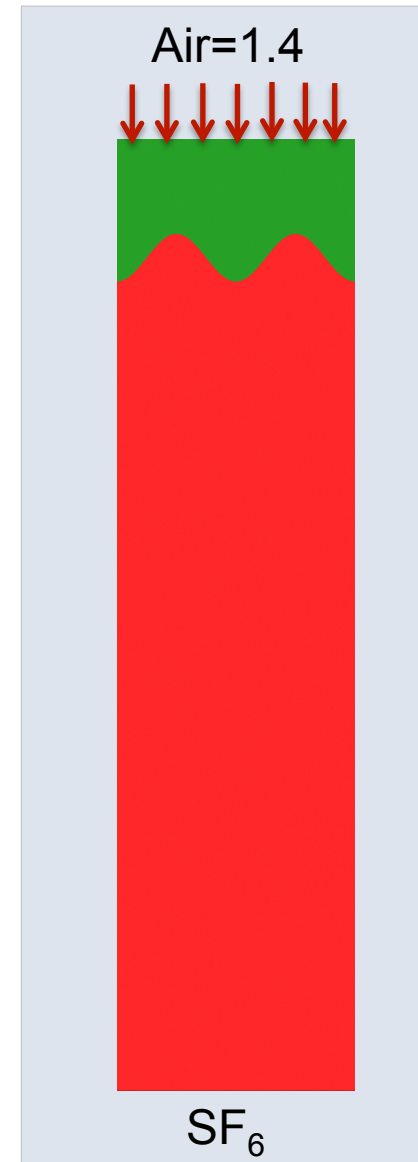
- Mesh: 100 nm, 20,000×80,000 = 1.6 billion cells
- Molecules: 800 billion molecules (500 per cell)
- Time steps: 200,000×0.01 ns = 2 μs

## Computational aspects

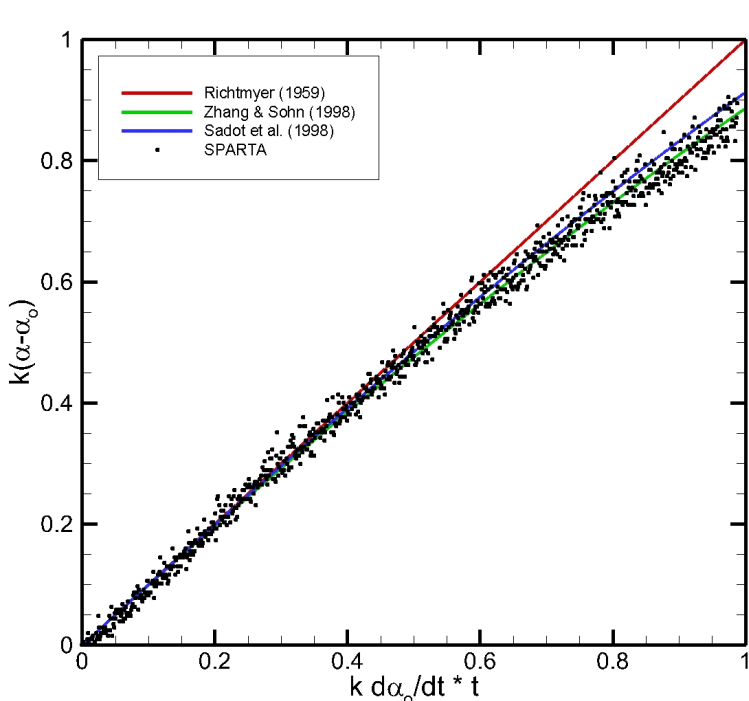
- Platform: Sequoia, 30 hours
- Processors: ~¼ million cores (16k nodes)

## Flow phenomena

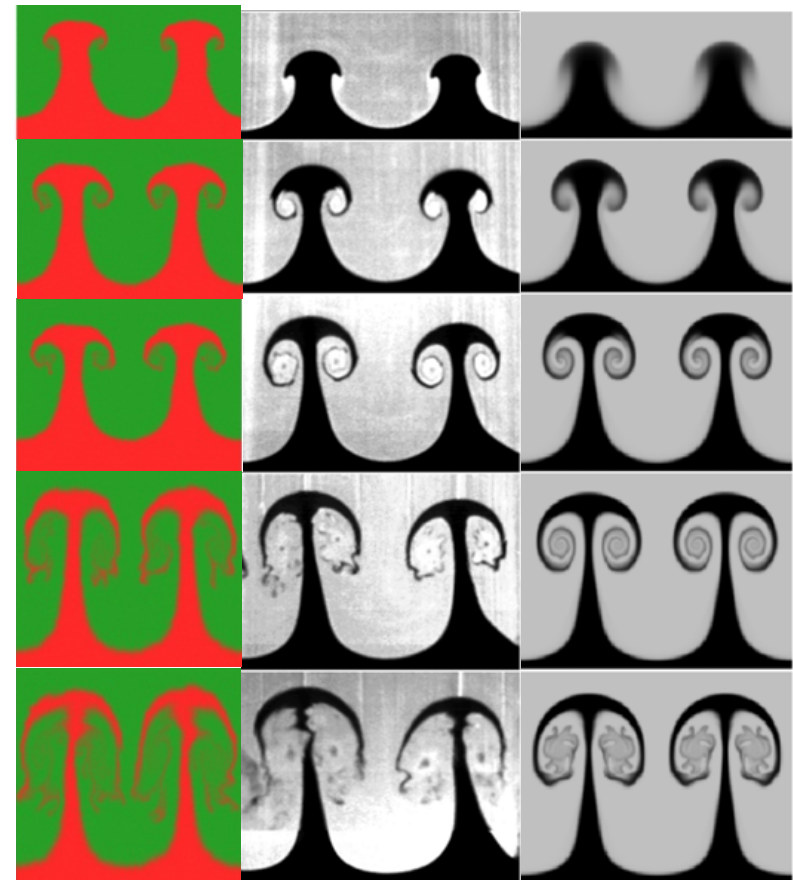
- Flow at top is impulsively started and maintained
- Shock wave propagates down and hits interface
- Transmitted and reflected shock waves depart
- Interface moves down and grows thicker



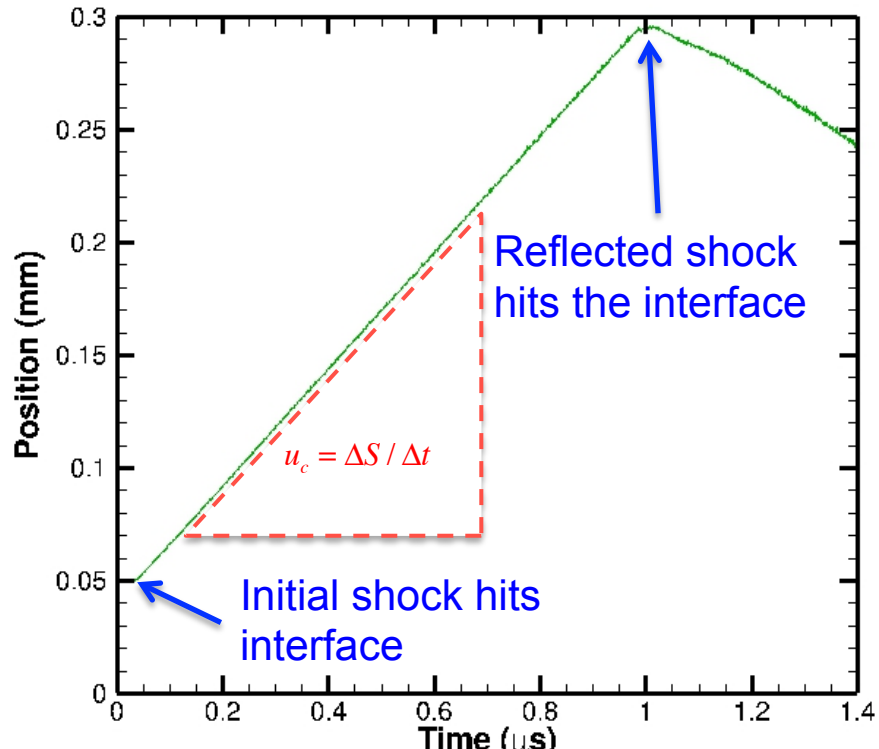
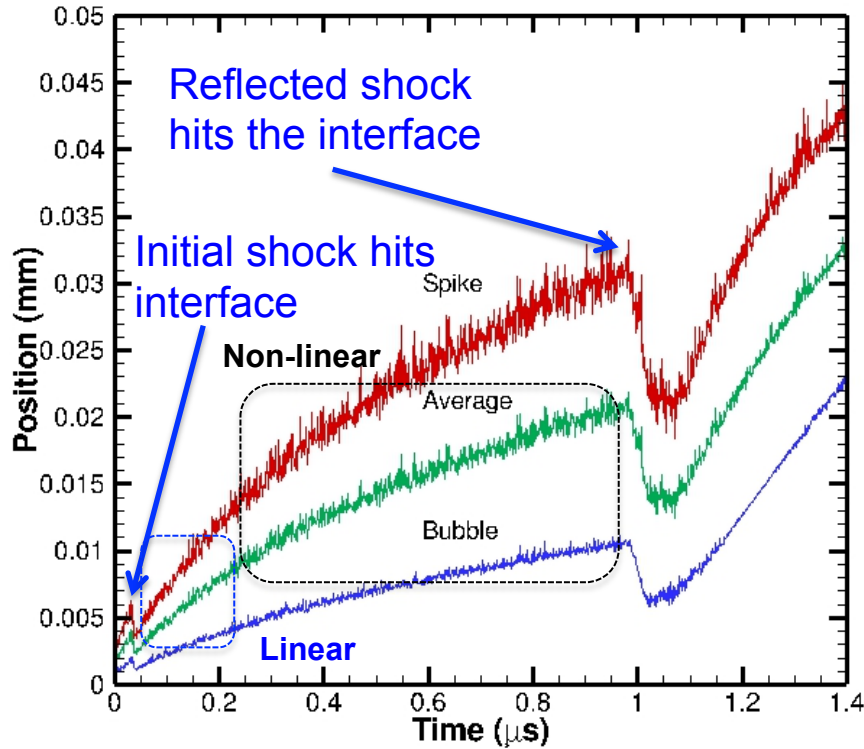
# RMI in Air-SF<sub>6</sub> Mixture: Mach = 1.4 Shock



DSMC      Experiment      Navier-Stokes



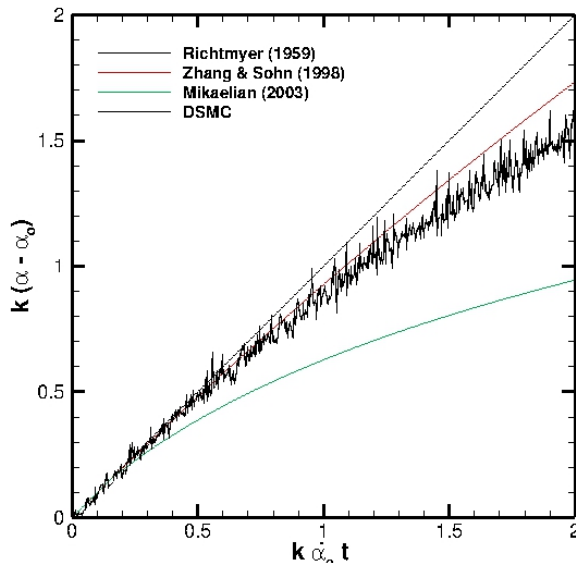
# Development of Bubbles and Spikes in RMI



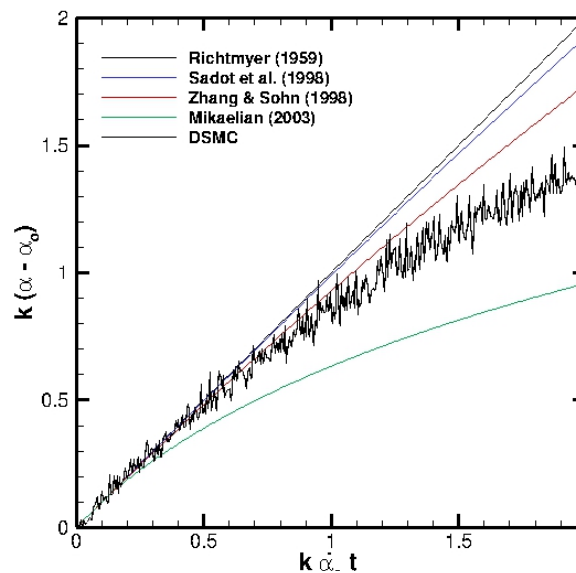
Interface moves with constant speed until the flow gets re-shocked  
The development of bubbles and spikes can be tracked independently

# DSMC-RMI Comparison to Theory

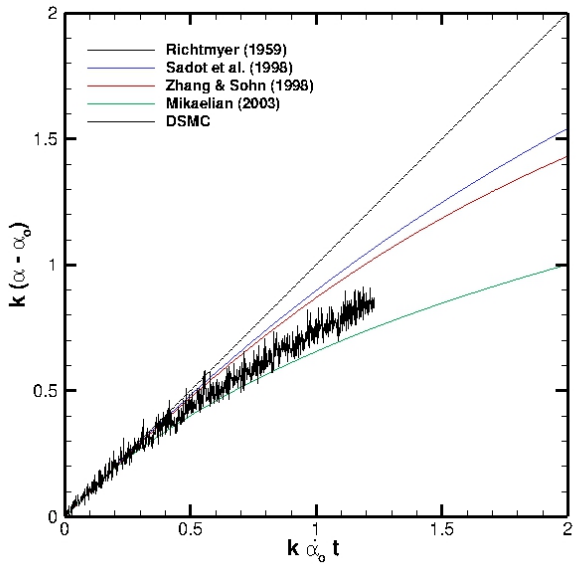
He/Xe  
A=0.94



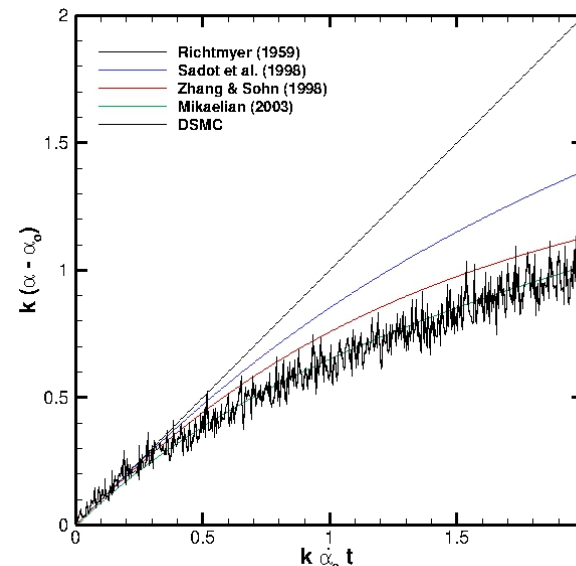
He/Ar  
A=0.61



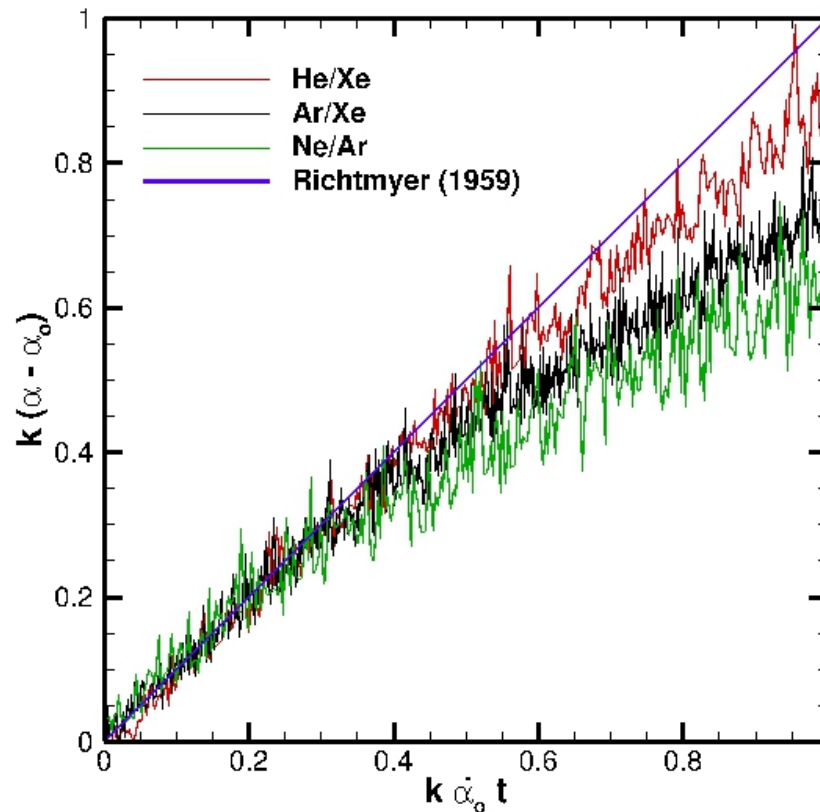
Ar/Xe  
A=0.53



Ne/Ar  
A=0.33

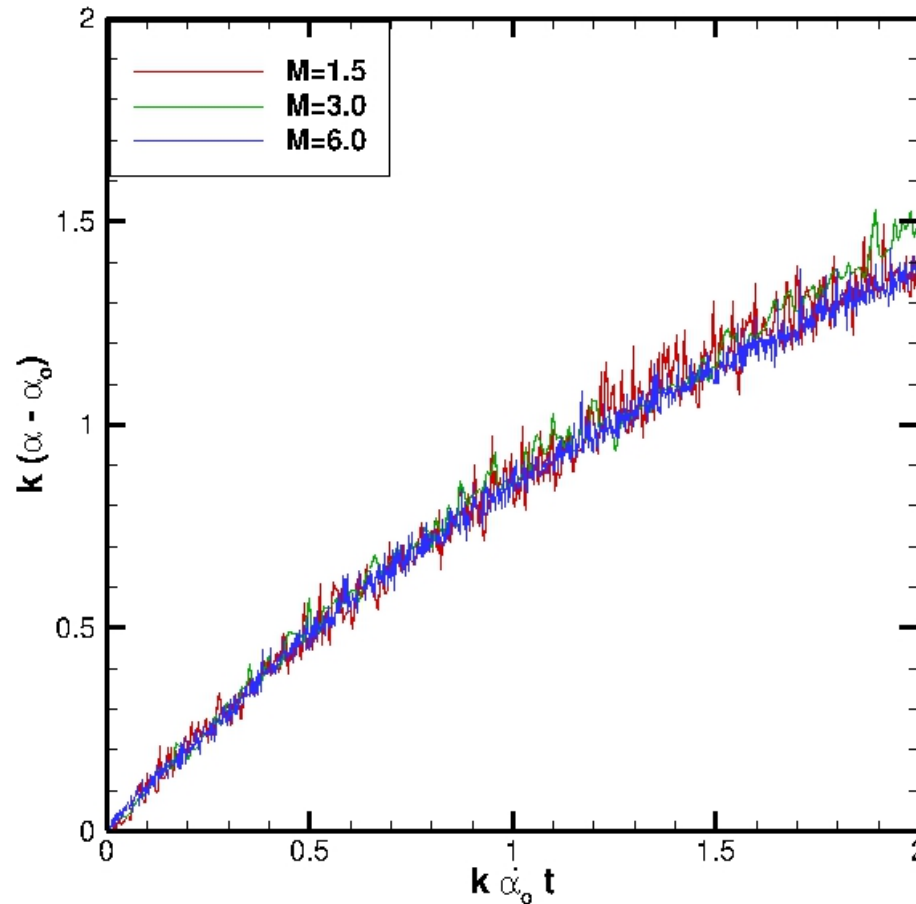


# RMI: Effect of Atwood Number



- Different gas pairs give different Atwood numbers in the range 0.329-0.941
- Modest differences are seen over the range examined

# RMI: Effect of Mach Number



Normalization indicates that Mach number plays a small role  
 None of the theoretical models accounts for Mach number

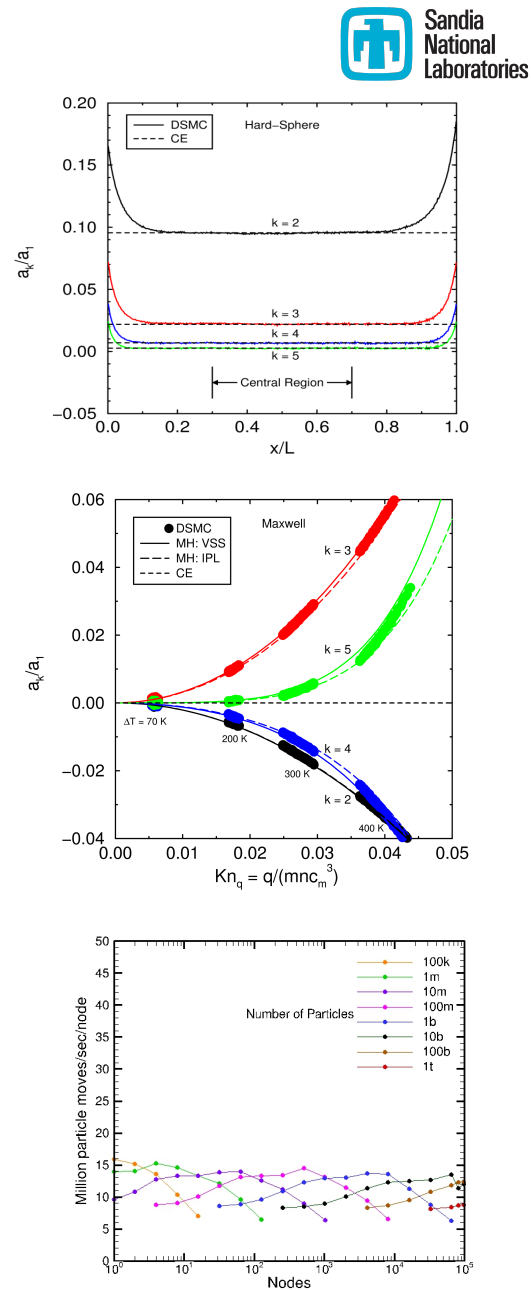
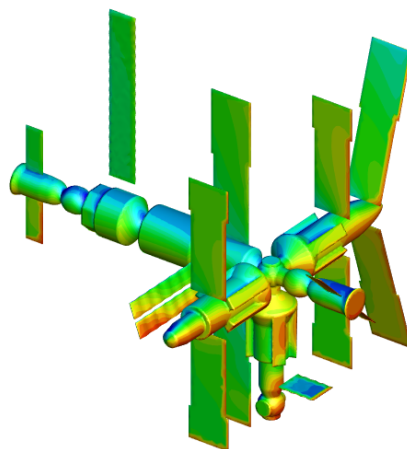
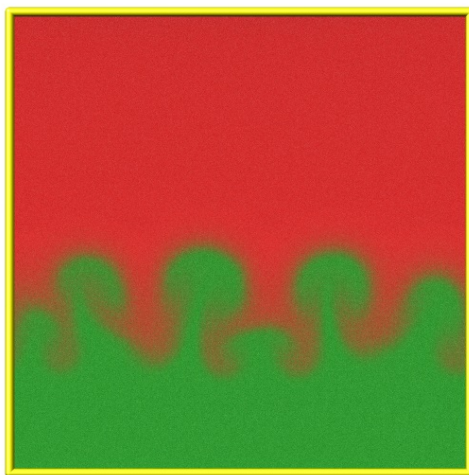
# Conclusions

DSMC yields exquisite agreement with analytical results, where available

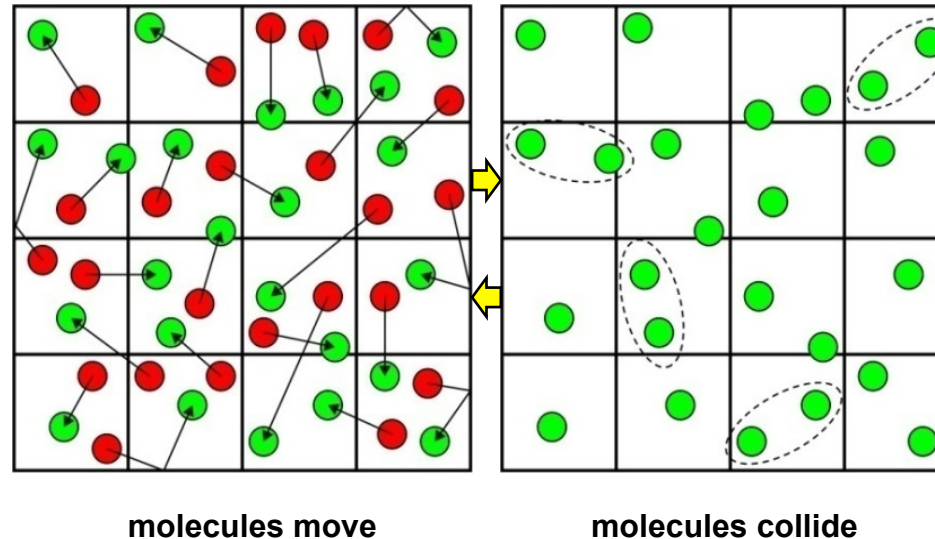
- Chapman-Enskog, Moment-Hierarchy theory

DSMC scales extremely well & can take full advantage of massively parallel platforms

- Can simulate unprecedented flow regimes
- Hydrodynamic instabilities, lower altitudes



# DSMC Numerical Error



Four parameters control DSMC error:

## Statistical error (1)

## Samples per cell ( $S_c$ )

## Discretization error (3)

- Particles per cell ( $N_c$ )
- Cell size ( $\Delta x$ )
- Time step ( $\Delta t$ )

# Statistical and Particle-Number Errors

## Error related to sample size

- Statistical error
- Cell sample size  $S_c = N_c \times N_t$
- $N_c$  = particles per cell;  $N_t$  = time steps

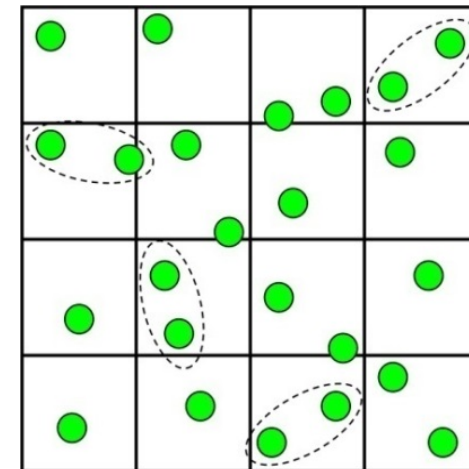
## Strategies for overcoming statistical error

- Use large number of samples
- For steady flows, use time and/or ensemble averaging
- Computational expense  $\sim S_c$

## Error related to local number of particles

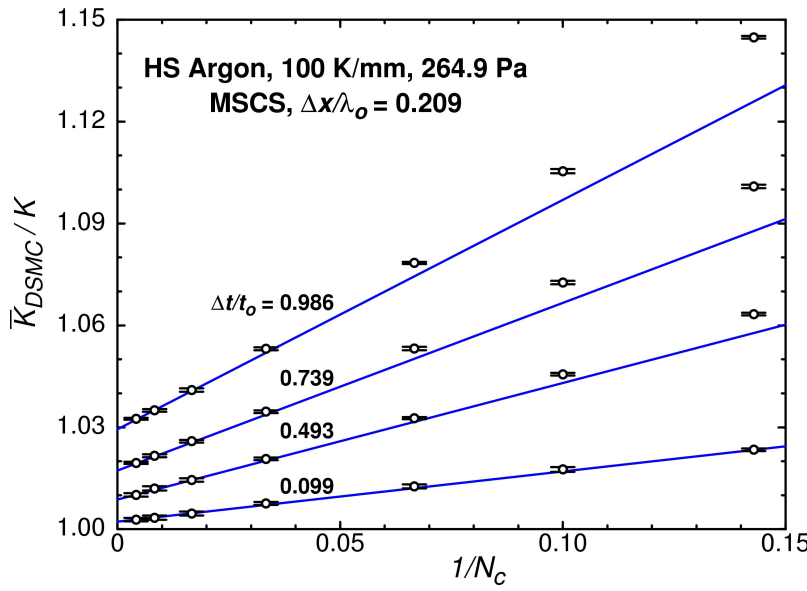
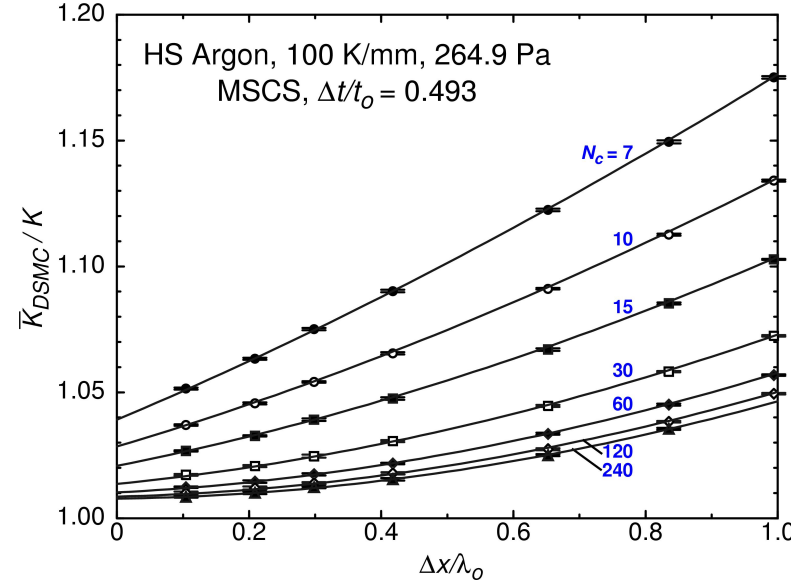
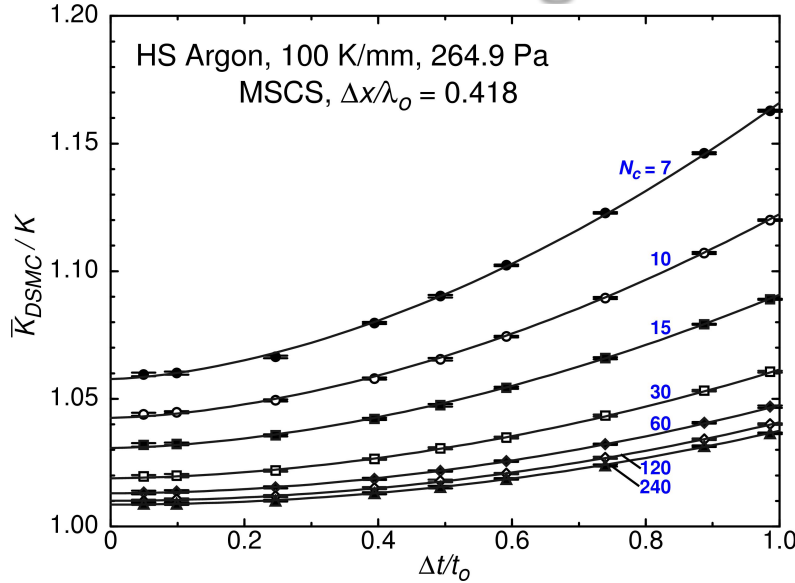
- Error  $\sim 1/N_c$
- Systematic – persists even as  $S_c \rightarrow \infty$

## Limited number of samples per time step



Not enough particles to capture physics

# DSMC Convergence



- Curves are best fits
- Error bars represent 95% confidence intervals
- Quadratic convergence for  $\Delta x, \Delta t$
- **First-order convergence**  $O(1/N_c)$ , as  $N_c \rightarrow \infty$
- Higher-order for long time steps
- For  $N_c = 7$  and  $\Delta t/t_o = 0.493$ , convergence rate appears linear in  $\Delta x/\lambda_o$

# Functional Form of Error

*Functional form that represents DSMC data*

- *Ad hoc* series expansion in  $\Delta x$ ,  $\Delta t$ , and  $1/N_c$
- Perform least-squares fitting of entire data set

$$\frac{K_{DSMC}}{K} = 1.0000 + 0.0286\tilde{\Delta t}^2 + 0.0411\tilde{\Delta x}^2 - 0.0016\tilde{\Delta x}^3 - 0.023\tilde{\Delta t}^2\tilde{\Delta x}^2 +$$

$$- \frac{0.111}{N_c} + \frac{1}{N_c} [1.22\tilde{\Delta x} - 0.26\tilde{\Delta x}^2 + 0.97\tilde{\Delta t}^{3/2} + \dots] + 0.95\frac{\tilde{\Delta t}^2}{N_c^2} + \dots$$

*Cross terms show convergence behavior is complex*

Rader D. J., Gallis M. A., Torczynski J. R., Wagner W., “DSMC Convergence Behavior of the Hard-Sphere-Gas Thermal Conductivity for Fourier Heat Flow”, *Phys. Fluids*, 18, 077102, 2006.

# DSMC Numerical Error

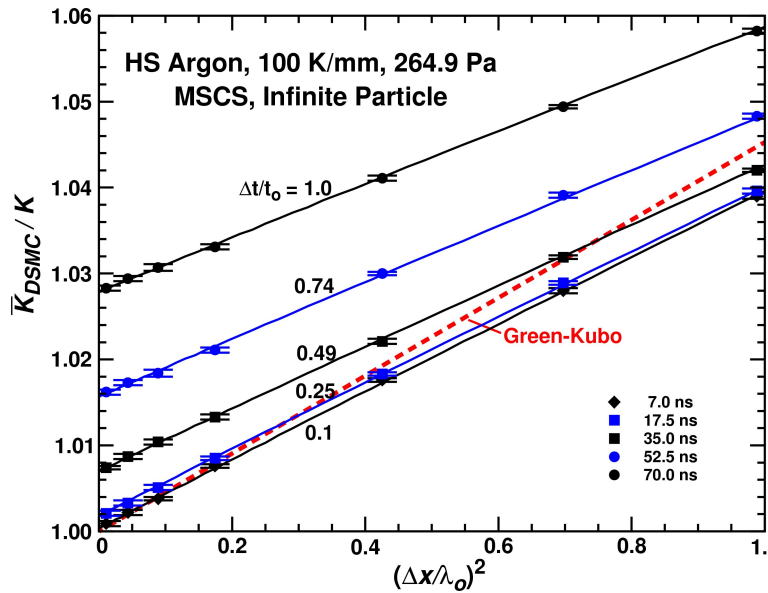
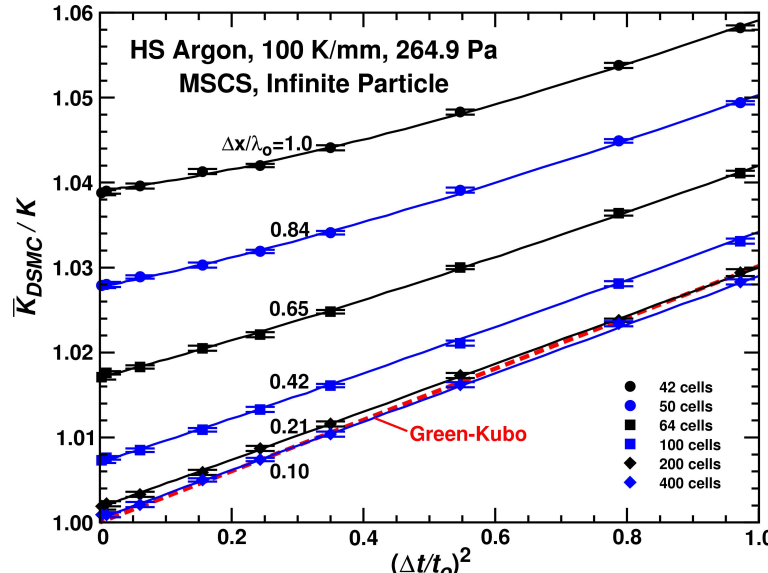
## Traditional DSMC rule-of-thumb guidelines:

- Take enough samples to drive statistical error down to “acceptable” level
- Keep time step smaller than  $\sim 1/4$  mean collision time
- Keep cell size smaller than  $\sim 1/3$  mean free path
- Use a minimum of  $\sim 20$  particles per cell

*These guidelines give 2% error, which is similar to the uncertainty in measured transport properties for most gases*

- DSMC is subject to the same constraints as other numerical methods.
- DSMC is correct to the limit of vanishing discretization.

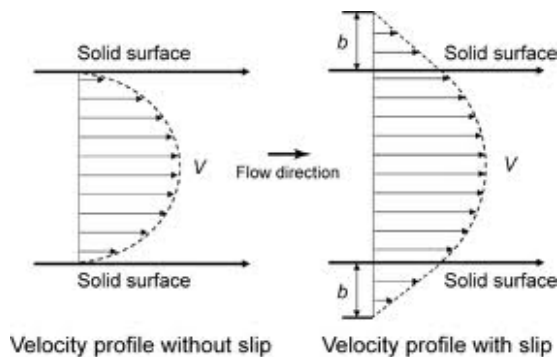
# Infinite-Particle Convergence



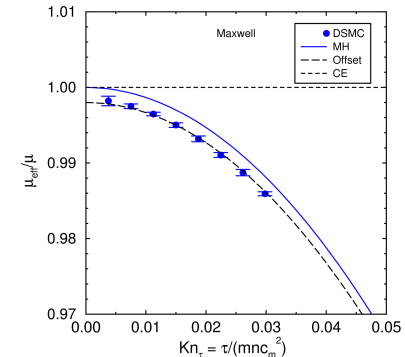
- Finite-particle error removed: values “extrapolated” to  $N_c \rightarrow \infty$
- 63 extrapolated data points
- Error bars: fitting uncertainty
- Quadratic convergence in time step and cell size
- Qualitative agreement with **Green-Kubo** theory, but slopes are different
- Lines are best fits of data

# Could the N-S Equations be extended ?

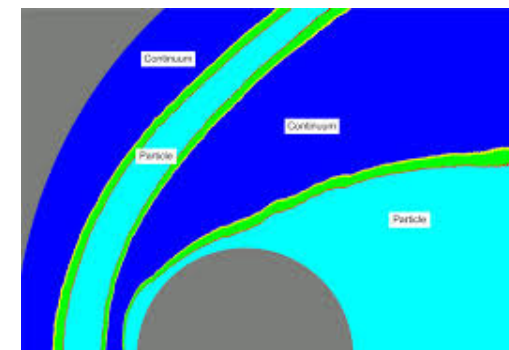
- Velocity-slip and Temperature jump



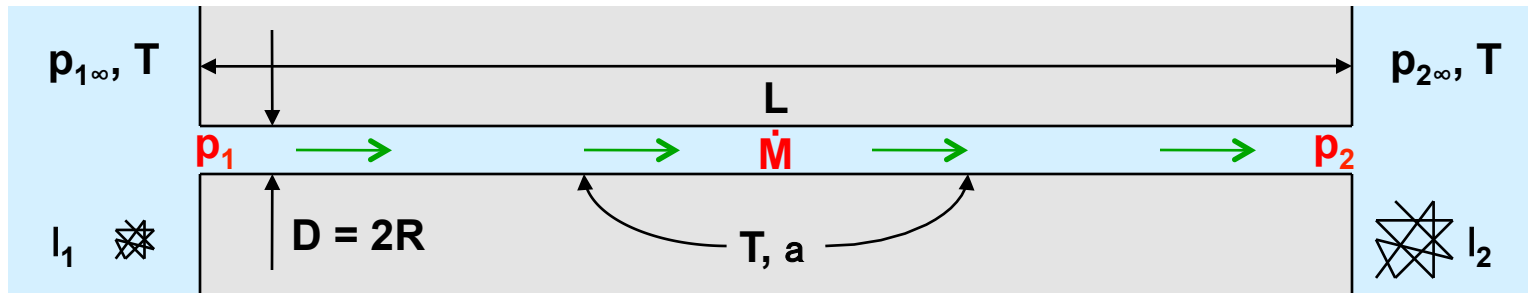
- Modified transport coefficients  
(viscosity, conductivity, diffusivity)



- Hybrid Schemes (NS-DSMC)



# Gas Flow in a Microscale Tube



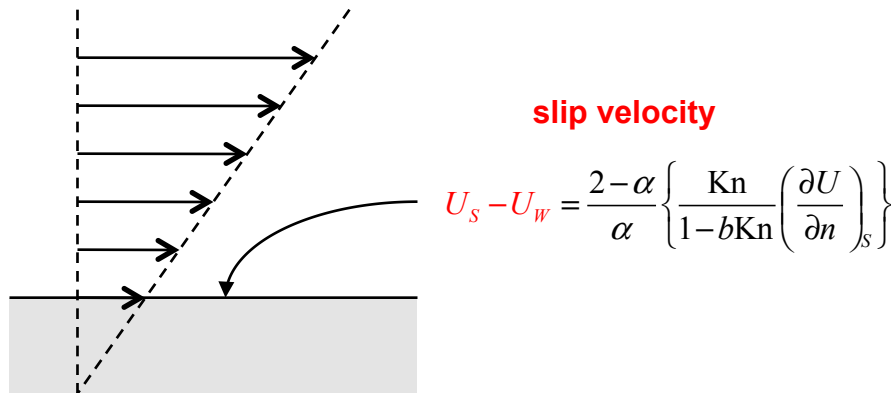
Investigate steady isothermal gas flow in microscale tube

- Tube is long and thin ( $L \gg D$ ) with circular cross section
- Tube joins gas reservoirs at different pressures ( $p_{1\infty} \geq p_{2\infty}$ )
- Tube and reservoirs have same temperature ( $T$ )
- Molecules partially accommodate ( $a \leq 1$ ) when reflecting
- Flow speed  $\ll$  molecule speed, laminar, no turbulence

Determine the mass flow rate and the pressure profile

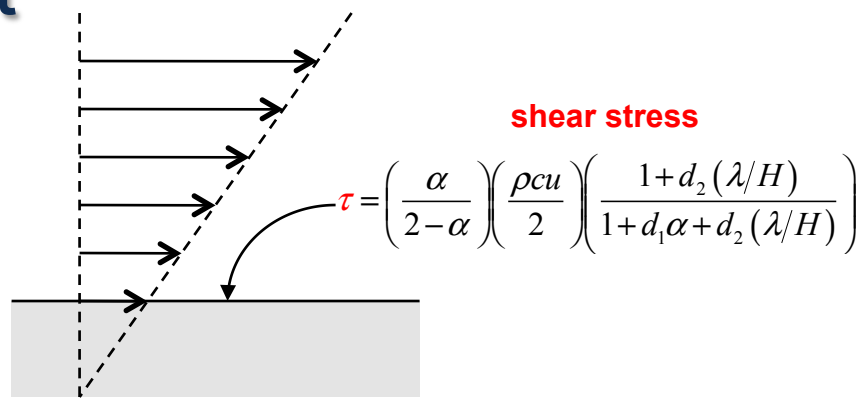
- General physics-based closed-form expressions
- Free-molecular to continuum (arbitrary mean free path  $l$ )
- Theory and molecular-gas-dynamics simulations

# Extending the Navier-Stokes equations



- Mean free path at STP is 0.06 mm, large enough to matter
- Silicon channels of  $<10 \mu\text{m}$  height and  $>10 \mu\text{m}$  length
  
- Accurate mass flow rate needs accurate velocity profile
- Slip boundary condition improves prediction by Navier-Stokes equations

# Boundary Conditions for Accurate Transport



- Transport rates are of primary importance
  - Mass, momentum, energy
- Fields are of secondary importance
  - Concentration, velocity, temperature

Construct boundary conditions to give accurate transport

- When used with Navier-Stokes equations
- For free-molecular, transition, slip, continuum

Resulting fields are only qualitatively correct

- Fields are accurate in continuum limit

# Mass Flow Rate Has Correct Limits

## Approximate Closed-Form Expression

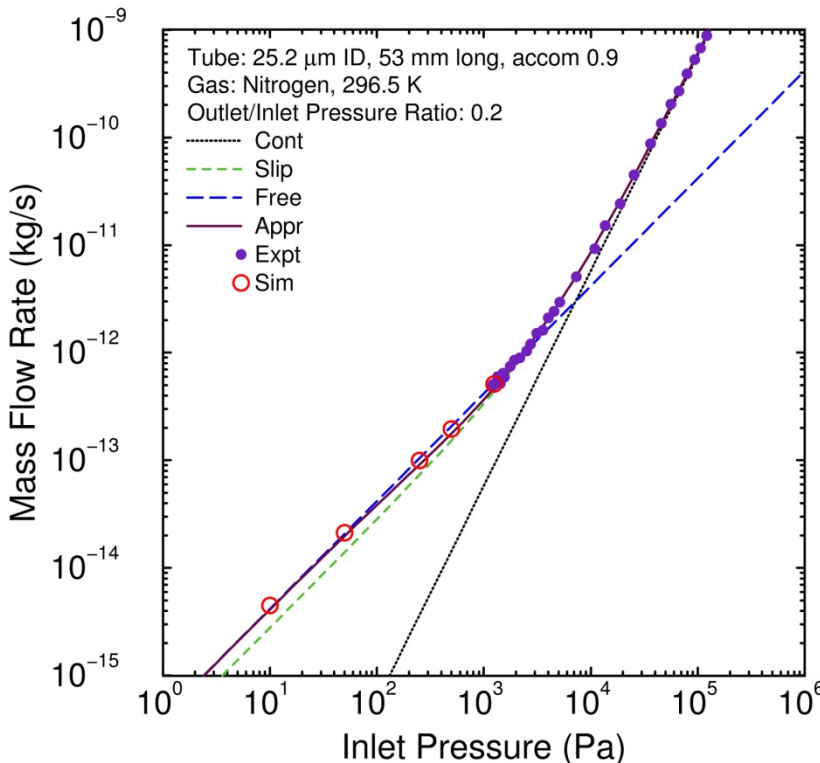
$$\dot{M} = \dot{M}_C \left( 1 + \frac{8p_\lambda}{p_m} \varpi [p_A, p_B] \right), \quad \varpi [p_A, p_B] = \frac{2-\alpha}{\alpha} \left\{ 1 + b_1 \alpha + (\varepsilon b_0 - 1 - b_1 \alpha) \frac{b_2 p_\lambda}{p_A - p_B} \ln \left[ \frac{p_A + b_2 p_\lambda}{p_B + b_2 p_\lambda} \right] \right\}$$

Continuum	Slip	Free-Molecular
$\dot{M}_C = \frac{D^4 p_m (p_1 - p_2)}{16 \mu c^2 L}$	$\dot{M}_S = \dot{M}_C \left( 1 + \frac{8p_\lambda}{p_m} \varpi_S \right), \quad \varpi_S = \frac{2-\alpha}{\alpha} (1 + b_1 \alpha)$	$\dot{M}_F = \dot{M}_C \left( \frac{8p_\lambda}{p_m} \varpi_F \right), \quad \varpi_F = \frac{2-\alpha}{\alpha} \varepsilon b_0$
Continuum Orifice	Free-Molecular Orifice	Free-Molecular Short Tube
$\dot{M}_{OC} = \frac{R^3 \rho_{m\infty}}{3\mu} (p_{1\infty} - p_{2\infty})$	$\dot{M}_{OF} = \pi R^2 \frac{mc}{4} (n_{1\infty} - n_{2\infty})$	$\dot{M}_{TF} = \dot{M}_{OF} / (1 + (\alpha L/D)), \quad \alpha L/D \ll 1$

Expression reproduces known limits correctly

Continuum	Not affected by $e$ , $b_0$ , $b_1$ , $b_2$
Slip	Determined by $b_1$
Free-Molecular	Determined by $e$ , $b_0$
Orifice/Short-Tube	Determined by $e$ , $b_0$

# Ewart et al. (2006) Tube Experiments



## Tube Mass Flow Rate

$$\dot{M} = \dot{M}_C \left( 1 + \frac{8p_\lambda}{p_m} \varpi[p_1, p_2] \right), \quad \dot{M}_C = \frac{D^4}{16} \frac{p_m(p_1 - p_2)}{\mu c^2 L}$$

$$\varpi[p_A, p_B] = \frac{2-\alpha}{\alpha} \left\{ 1 + b_1 \alpha + (\varepsilon b_0 - 1 - b_1 \alpha) \frac{b_2 p_\lambda}{p_A - p_B} \ln \left[ \frac{p_A + b_2 p_\lambda}{p_B + b_2 p_\lambda} \right] \right\}$$

$$\rho = \frac{mp}{k_B T}, \quad \mu = \mu[T], \quad c = \sqrt{\frac{8k_B T}{\pi m}}, \quad \lambda = \frac{2\mu}{\rho c}, \quad p_\lambda = \frac{p\lambda}{D}, \quad p_m = \frac{p_1 + p_2}{2}, \quad \text{Kn}_m = \frac{p_\lambda}{p_m}$$

$$\frac{\alpha L}{D} > 10^3, \quad \varepsilon \rightarrow 1, \quad p_1 \rightarrow p_{1\infty}, \quad p_2 \rightarrow p_{2\infty}; \quad b_0 = \frac{16}{3\pi}, \quad b_1 = 0.15, \quad b_2 = \frac{0.7\alpha}{2-\alpha}$$

Same values of  $\varepsilon$ ,  $b_0$ ,  $b_1$ ,  $b_2$  used for all circular tubes

Values are unchanged from previous cases (no adjusting)  
Relative to diameter, this tube length is essentially infinite

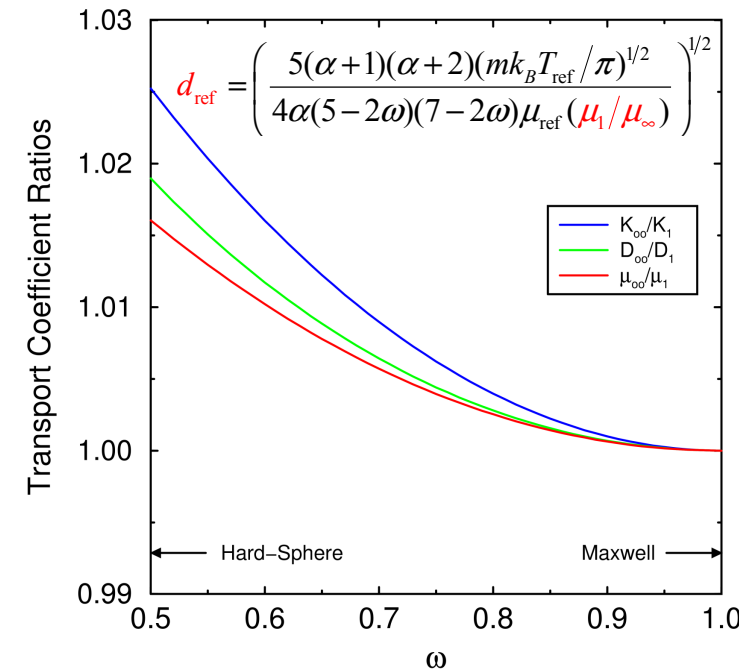
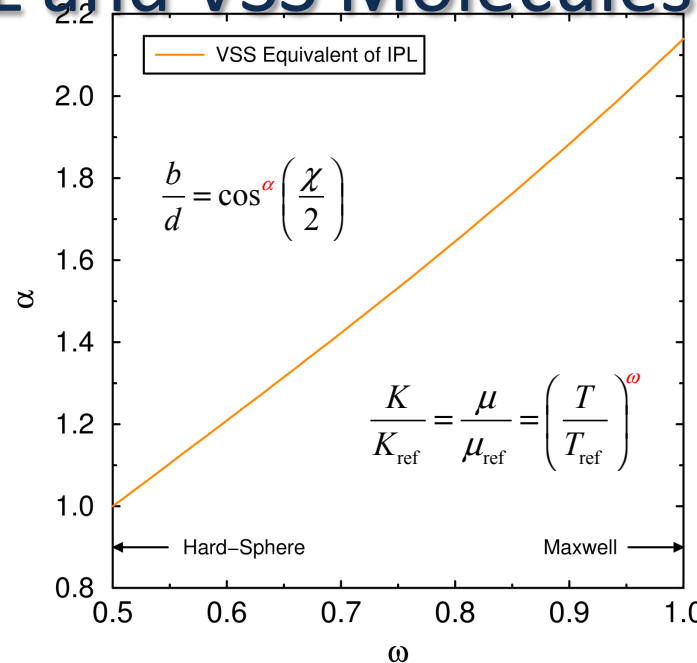
Mass flow rate measured for silica microscale tube

- $D = 25.2 \text{ mm}$ ,  $L = 53 \text{ mm}$ ,  $a = 0.9$ ,  $\text{N}_2$ ,  $T = 296.5 \text{ K}$ ,  $p_2/p_1 = 0.2$

Expression and simulations agree well with experiment

- Lowest experiment pressure is above Knudsen minimum
- Highest simulation pressure reaches experiment

# IPL and VSS Molecules



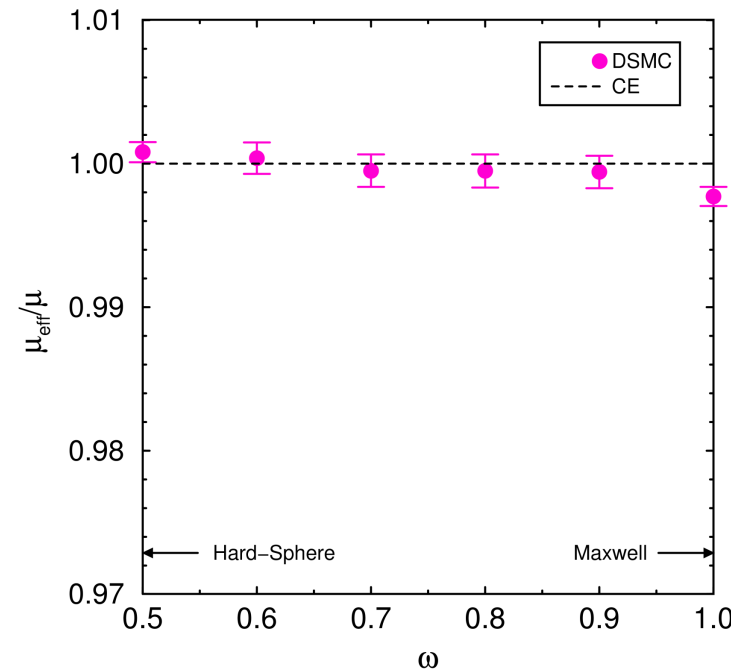
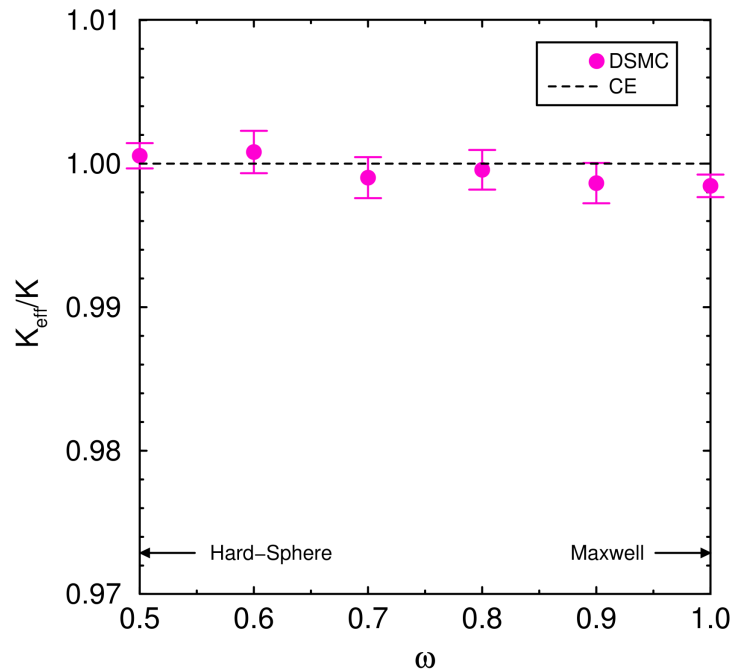
Best VSS  $w, a$  to match IPL  $w$  by equating diffusivities

- Identical match only for hard-sphere
- VSS-Maxwell  $\neq$  IPL-Maxwell (they are very similar)

Infinite-approximation CE changes  $K$  and  $m$  by  $O(0.03)$

- Affects reference diameter  $d_{\text{ref}}$  very slightly

# Transport Coefficients

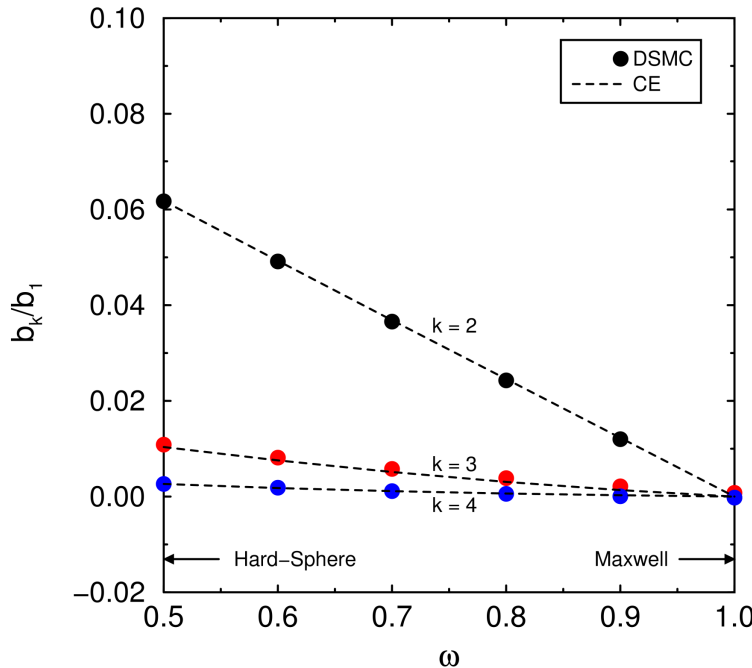
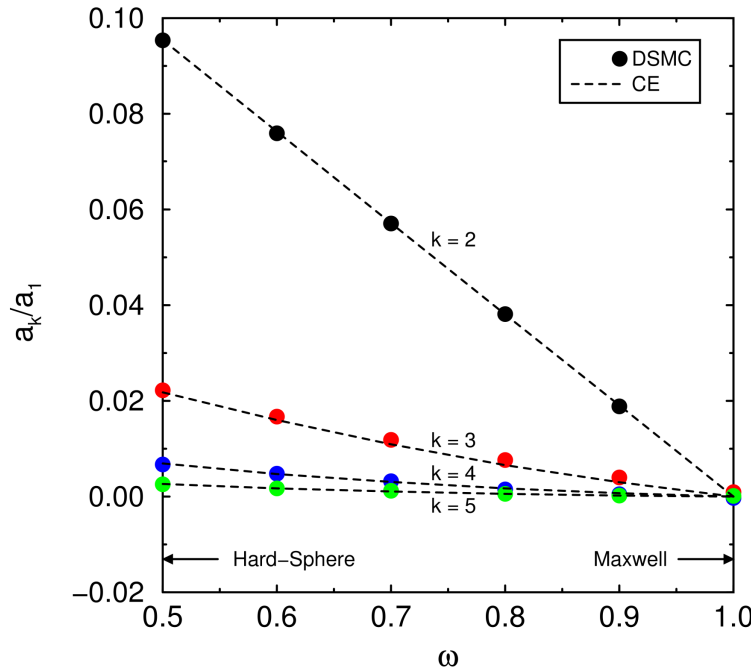


## Thermal conductivity and viscosity for IPL molecules

- Intermolecular force: hard-sphere through Maxwell
- Stochastic and discretization errors:  $\pm 0.002$  each
- CE infinite-to-first-approximation difference:  $O(0.03)$

Excellent agreement between DSMC and CE

# Sonine Coefficients



## Sonine coefficients $a_k/a_1$ and $b_k/b_1$ for IPL molecules

- Intermolecular force: hard-sphere through Maxwell
- Stochastic, discretization errors: smaller than symbols

## Good agreement between DSMC and CE

- Higher- $k$  coefficients have similar agreement
- Slight difference for  $k = 3$ ,  $\text{Kn}_q$  not small enough